ARTICLES
https://doi.org/10.1038/s41559-019-1070-4
nature ecology & evolution

Macroevolutionary convergence connects morphological form to ecological function in birds

Alex L. Pigot[1,2,13*], Catherine Sheard[2,3,13], Eliot T. Miller[4,5], Tom P. Bregman[2,6], Benjamin G. Freeman[7], Uri Roll[2,8], Nathalie Seddon[2], Christopher H. Trisos[2,9], Brian C. Weeks[10,11] and Joseph A. Tobias[2,12*]

Animals have diversified into a bewildering variety of morphological forms exploiting a complex configuration of trophic niches. Their morphological diversity is widely used as an index of ecosystem function, but the extent to which animal traits predict trophic niches and associated ecological processes is unclear. Here we use the measurements of nine key morphological traits for >99% bird species to show that avian trophic diversity is described by a trait space with four dimensions. The position of species within this space maps with 70–85% accuracy onto major niche axes, including trophic level, dietary resource type and finer-scale variation in foraging behaviour. Phylogenetic analyses reveal that these form–function associations reflect convergence towards predictable trait combinations, indicating that morphological variation is organized into a limited set of dimensions by evolutionary adaptation. Our results establish the minimum dimensionality required for avian functional traits to predict subtle variation in trophic niches and provide a global framework for exploring the origin, function and conservation of bird diversity.

Plants and animals have complementary functions in the biosphere, with plants mainly contributing as autotrophic producers and animals occupying multiple higher trophic levels as primary, secondary and tertiary consumers[1–4]. Restriction of most plant species to the foundation of food webs theoretically limits the scope for trophic niche variation, perhaps explaining why their vast trait diversity is predominantly constrained to a simple plane with two dimensions[5]. In contrast, the trait space associated with foraging niches in heterotrophic consumers is potentially more complex and multidimensional[6–9], particularly if distinct sets of morphological traits are consistently associated with different trophic levels and dietary types—including herbivores, pollinators and predators[10]. This concept of a predictable link between animal form and function has existed since Aristotle[11] and now underpins numerous trait-based research programmes[12], from resolving the evolutionary origins of biodiversity[13,14] to quantifying ecosystem function[15,16] and predicting responses to environmental change[17,18]. However, the assumption that ecological niche space and associated ecosystem functions can be adequately quantified using a limited set of phenotypic traits is controversial[19,20].

At one extreme of complexity, species and their traits may be embedded within an abstract multidimensional niche space, Hutchinson's *n*-dimensional hypervolume[21]. By assuming an almost limitless number of ecological dimensions, this model provides a compelling explanation for the diversity of species and phenotypes found in nature[13,14,21]. At the other extreme, the mapping of traits onto niche space may be simplified to a single dimension[22–24] by functional trade-offs[25] or pervasive convergent evolution[26,27]. Whether form–function relationships are either unfathomably complex or unexpectedly simple has major implications for the usefulness of trait-based approaches to quantifying and conserving biodiversity[16,28,29].

In a high-dimensional Hutchinsonian niche space, pinpointing the functional role of a species would require numerous axes of phenotypic variation[30], potentially confounding efforts to understand niches based on standardized trait datasets[12,15,17,18]. Conversely, if most of the diversity in functional traits can be collapsed along one or two fundamental dimensions, then this may not provide sufficient traction for traits to be informative about multiple ecological functions, particularly in multitrophic systems[19,28]. Some ecomorphological analyses have found evidence that the dimensionality of animal hypervolumes may lie somewhere between these extremes[30–32], raising hope that trait combinations could be partitioned into a relatively simple niche classification system, which is analogous to the periodic table of elements[27]. Yet, previous studies have focused on restricted spatial and taxonomic scales, producing contradictory results and no clear consensus about the structure or generality of form–function relationships in animals[31–36].

In this study, we present a comprehensive assessment of phenotypic trait diversity for extant birds (Aves), the largest class of tetrapod vertebrates. For over a century, birds have played a central role in the development of niche concepts and ecomorphology[31,37–39] and now provide the richest template for exploring the function and evolution of morphological traits in the context of species-level ecological[40] and phylogenetic datasets[41]. We measured eight phenotypic traits with well-established connections to locomotion, trophic ecology and the associated niche structure of ecological communities[31,32,39,42] (Extended Data Fig. 1; see Methods).

[1]Centre for Biodiversity and Environment Research, Department of Genetics, Evolution and Environment, University College London, London, UK. [2]Department of Zoology, University of Oxford, Oxford, UK. [3]School of Biology, University of St Andrews, St Andrews, UK. [4]Cornell Lab of Ornithology, Ithaca, NY, USA. [5]Department of Biological Sciences, University of Idaho, Moscow, ID, USA. [6]Future-Fit Foundation, London, UK. [7]Biodiversity Research Centre, University of British Columbia, Vancouver, British Columbia, Canada. [8]Mitrani Department of Desert Ecology, Jacob Balaustein Institutes for Desert Research, Ben-Gurion University of the Negev, Beer-Sheva, Israel. [9]African Climate and Development Initiative, University of Cape Town, Cape Town, South Africa. [10]School for Environment and Sustainability, University of Michigan, Ann Arbor, MI, USA. [11]Department of Ornithology, American Museum of Natural History, New York, NY, USA. [12]Department of Life Sciences, Imperial College London Silwood Park, Ascot, UK. [13]These authors contributed equally: Alex L. Pigot, Catherine Sheard. *e-mail: a.pigot@ucl.ac.uk; j.tobias@imperial.ac.uk

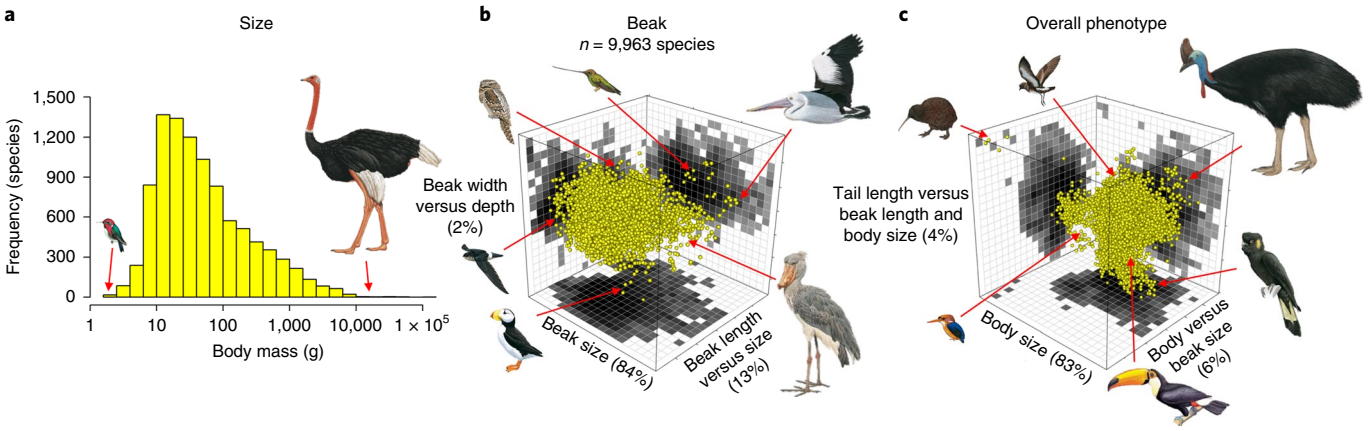

Fig. 1 | The avian morphospace. a, Distribution of avian body masses from the lightest (*Mellisuga helenae*, 2 g) to the heaviest species (*Struthio camelus*, 111 kg). **b**, Variation in beak shape, a key trait related to resource use. The first three dimensions of beak space capture variation in beak size (PC1), relative beak length (PC2) and ratio of beak depth to width (PC3). **c**, A three-dimensional morphospace combining data on body mass, beak, wing, tail and tarsus. The axes labels indicate the proportion of variance explained. The density of species is projected onto each two-dimensional plane. Data are shown for 9,963 species, representing >99% of all birds. Bird images reproduced with permission from HBW, Lynx Edicions.

In particular, the beak is the primary apparatus used by birds to capture and process food[39,43], while morphological differences in wings, tails and legs are related to locomotion, providing insight into the way birds move through their environment and forage for resources[31]. With the addition of body mass, our dataset contains full sets of 9 traits for 9,963 species, representing >99% of extant bird diversity and all 233 avian families (Supplementary Table 1), thereby summarizing whole-organism trait combinations in unprecedented detail for a major radiation of organisms distributed worldwide across marine and terrestrial biospheres. We use a range of analyses to explore the structure of this trait diversity and its connection to ecological function.

Results

The multiple dimensions of avian trait space. Across birds, body mass varies by a factor of 50,000 (Fig. 1a) and the position of species along this single axis has important associations with metabolism and life history[44]. To go beyond this basic variation among organisms, we can visualize avian trait diversity by projecting species into a multivariate space (hereafter, morphospace) derived from principal component scores (see Methods). These projections can be restricted to the beak (Fig. 1b and Supplementary Table 2) or expanded to encompass all traits (Fig. 1c and Supplementary Table 3), in both cases revealing enormous variation in size (principal component 1 (PC1)) and shape (PC2 and PC3).

Unlike the bimodal distribution of plant forms[5], variation in bird traits is centred on a single dense core around which species with extreme morphologies are scattered at the periphery of morphospace (Fig. 1b,c and Extended Data Figs. 3 and 4). The structure of these three-dimensional projections highlights the diverse ways birds have explored different trait combinations. For instance, the second dimension of total trait variation (PC2; 6% of trait variance) describes the spectrum from small to large beaks, while the third dimension (PC3; 4% of trait variance) separates species with short tails and pointed beaks (for example, kiwis) from those with long tails and stubby beaks (for example, frogmouths) (Extended Data Fig. 3). Compared to the primary axis of body size (PC1), along which most (83%) phenotypic variation is aligned, these and the remaining dimensions of avian morphospace constitute only a fraction of total phenotypic variation (17%). However, the key question is whether the position of species in this high-dimensional morphospace provides deeper insight into their ecological function.

Mapping form to function. To understand how morphology relates to ecological function, we classified species into different types of primary consumers (aquatic and terrestrial herbivores, nectarivores, frugivores, granivores), secondary and tertiary consumers (aquatic and terrestrial carnivores) and scavengers (Extended Data Fig. 5a; see Methods). We further separated terrestrial carnivore niches into vertivores (consumers of vertebrates) and invertivores (consumers of invertebrates). Most avian species are largely specialized on a single trophic level ($n = 8{,}343$ species) and, within this, a single trophic niche ($n = 8{,}229$ species). The rest constitute omnivores that exploit multiple trophic levels ($n = 1{,}620$ species) or niches (either within or across levels, $n = 1{,}734$ species) in relatively equal proportions (see Methods). To test whether the location of species in morphospace predicts their trophic niche, we used a random forest model, a type of machine learning algorithm that applies recursive partitioning (that is, decision trees) to subdivide morphospace into a set of non-overlapping rectangular hypervolumes within which variation in species niches is minimized (see Methods). We began by assessing whether body mass alone can predict species' trophic niche, then added additional traits to build up a progressively more complete description of avian phenotype.

We found that a model using only body mass (Fig. 2a) achieved only limited accuracy in predicting either trophic niches (29%) or broad trophic levels (38%). Only nectar-feeding pollinators—many of which, including hummingbirds (Trochilidae), have evolved miniaturized forms to feed on flowers—were predicted consistently by body mass (Fig. 2b). Thus, although body size accounts for most of the variance in our phenotypic traits (Supplementary Table 3), it provides a relatively weak explanation of avian trophic niche space at global scales. The predictability of trophic niches more than doubled when beak size and shape were included (Fig. 2a,c) and increased further to 78% when we used a nine-dimensional morphospace with a full set of beak and body traits (Fig. 2a,d). Moreover, when we excluded omnivores (see Methods), thereby restricting the analysis to species with the most specialized diets, the predictability of trophic niches and trophic levels exceeded 80% (Fig. 2a). These results were robust to the method used to match traits and ecology, with alternative approaches (for example, discriminant analysis) indicating a similar rise in predictive accuracy as morphological dimensionality increases (Extended Data Fig. 6; see Methods).

To visualize the striking connection between phenotypic form and trophic function, we mapped the density of each specialist trophic niche onto morphospace ($n = 8{,}229$). Even when projected onto a two-dimensional plane, as defined by beak size and shape,

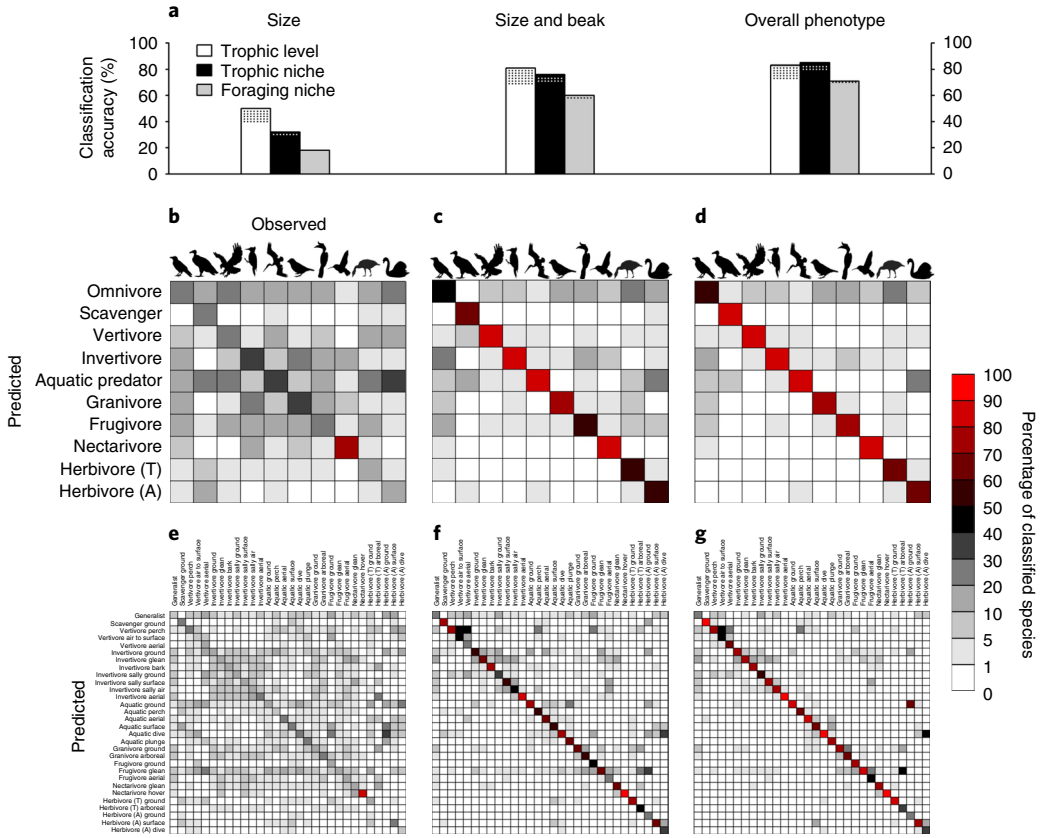

Fig. 2 | Trophic structuring of multidimensional morphospace. a, Mean accuracy (%) of a random forest model predicting trophic level, trophic niche and foraging niche for all birds ($n = 9{,}963$ species) on the basis of body size (mass), size and beak traits, or the full nine-dimensional morphospace. Stippling indicates improvement in predictive accuracy after omitting omnivores (see Methods). **b**–**g**, Confusion matrices show predictions for each trophic (**b**–**d**) and foraging niche (**e**–**g**) on the basis of body size (**b**,**e**), body size and beak (**c**,**f**), and overall phenotype (**d**,**g**). The diagonal elements of each matrix indicate correct matches between predicted and observed niches; off-diagonal elements indicate misclassification. Red, high levels of accuracy (diagonal) or misclassification (off-diagonal). Bird images reproduced with permission from HBW, Lynx Edicions.

it is clear that each trophic level, and indeed each trophic niche, occupies a largely distinct region of morphospace (Fig. 3). Specialist invertivores ($n = 4{,}765$ species) and frugivores ($n = 1{,}030$ species) constitute the bulk of avian species diversity and are diffusely distributed around the centre of morphospace (Fig. 3f,g). Species targeting other resource types possess more extreme combinations of beak size and shape, forming tighter clusters around the periphery (Fig. 3a–e,h,i and Extended Data Fig. 4). These clusters have irregular shapes but generally occupy a single contiguous region of morphospace—a 'phenotypic fingerprint'—concentrated around a unique central peak of high species density. This relatively simple one-to-one mapping of form to function is not an artefact of projecting niches onto a single two-dimensional plane because even in the full nine-dimensional morphospace each trophic niche can be well described by just one or a few rectangular hypervolumes (see Methods).

The ecological relevance of trait variation may extend far beyond predictions of simple trophic niches if morphology captures additional axes of ecological divergence, including subtle gradations of behaviour and microhabitat. The intrinsic subdivision of basic trophic niches into numerous variants is best illustrated in birds by terrestrial invertivores that have evolved a remarkable array of foraging techniques, from catching insects in continuous flight (for example, swallows) to plucking them from vegetation (for example, antshrikes) or hopping on the ground (for example, pittas) (Fig. 4 and Extended Data Fig. 5b). To assess how morphology relates to these finer-scale aspects of the niche, we reran the random forest model after subdividing the 9 specialist trophic niches into 30 foraging niches (Fig. 2e–g and Supplementary Table 4; see Methods).

As expected, foraging niches are even less predictable than trophic niches or trophic levels on the basis of body size (Fig. 2a). However, predictability increases substantially when using multiple trait dimensions, with the location in nine-dimensional morphospace accurately predicting not only the type of resources, but also the specific foraging manoeuvre and substrate used by each species (Fig. 2a,e–g). This result shows that most morphological variation encompassed by each trophic niche (Fig. 3) is not simply redundant[35,36], with numerous different combinations of traits performing similar ecological roles[8]. Instead, the striking correspondence between avian form and function provides continuous metrics for quantifying multitrophic niches with much greater detail and precision than afforded by coarse ecological categories.

Dimensionality of trophic niche space. To investigate the minimum number of dimensions required to predict avian niches, we applied random forest models to morphospaces of varying dimensionality, ranging from 1 to 9 dimensions, exploring all possible combinations of trait axes ($n = 511$ combinations). Based on estimates of model predictive accuracy, we then calculated the dimensionality (D) of trophic niches using Levene's index (see Methods). According to this index, $D = 9$ if all trait dimensions contribute equally to predicting trophic niches, with D decreasing towards 1 as predictive accuracy is driven by progressively fewer trait dimensions. Using this approach, we calculated the overall dimensionality

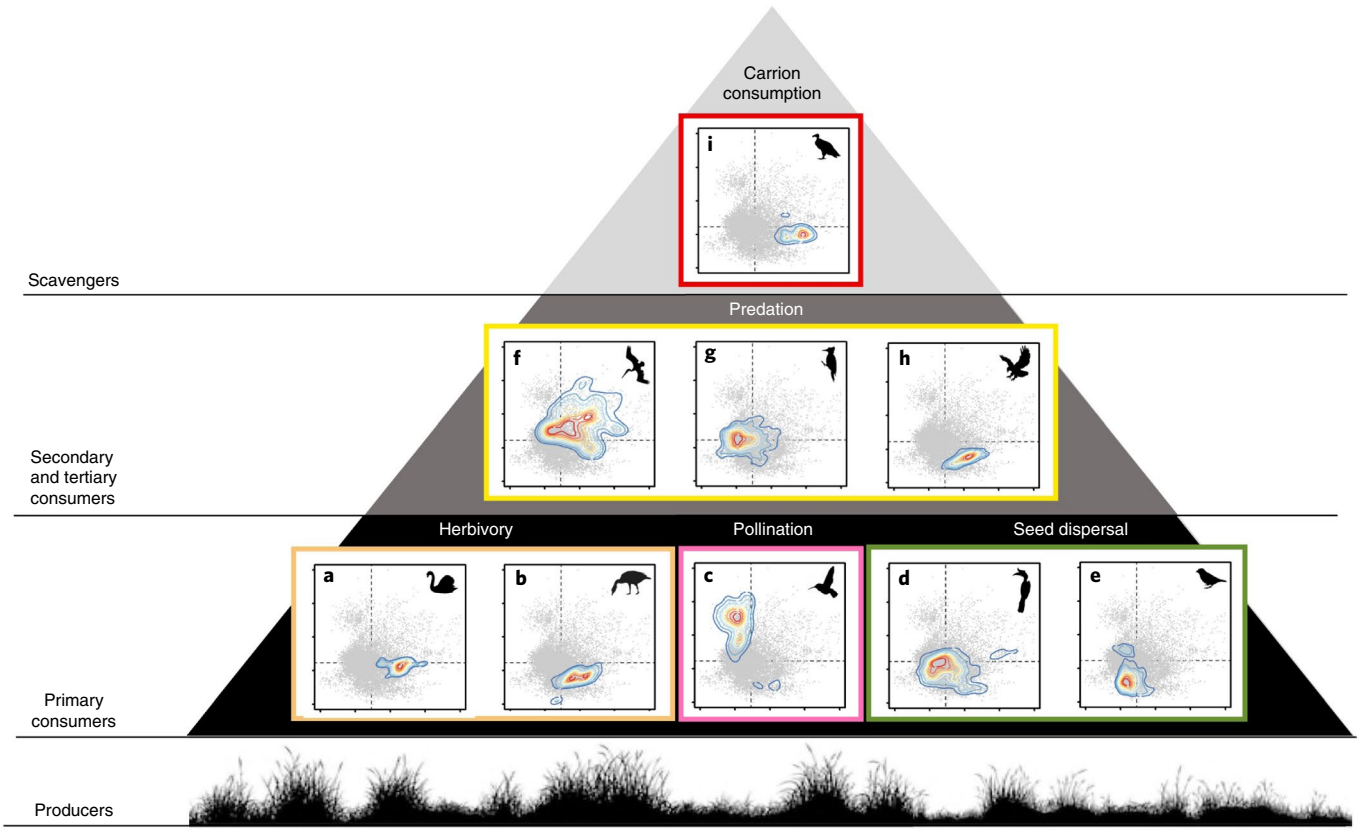

Fig. 3 | Partitioning of avian morphospace across trophic levels and niches. a–i, Heterotrophic consumers shape the biosphere through numerous feedbacks on nutrient cycling and productivity[2]. An illustration of the complexity of avian ecological function as a multitrophic pyramid built on a foundation of autotrophic producers (plants), which are exploited directly by aquatic herbivores (**a**), terrestrial herbivores (**b**), nectarivores (**c**), frugivores (**d**) and granivores (**e**), and indirectly by aquatic carnivores (**f**), terrestrial invertivores (**g**), terrestrial vertivores (**h**) and scavengers (**i**). Within each trophic niche, the first two dimensions of beak morphospace, capturing variation in beak size (PC1) and shape (PC2), are plotted against total beak variation of 9,963 species, representing >99% of all birds (light grey). The contours indicate species density; the warmer colours indicate higher density. Omnivores are not shown. Bird images reproduced with permission from HBW, Lynx Edicions.

of trophic niche space (D_{Total}) as well as the mean dimensionality across individual trophic niches ($\bar{D}$).

We found that dimensionality varied from the two-dimensional niche of nectarivores to the four-dimensional niche of frugivores, and that niches are on average defined by at least three trait dimensions ($\bar{D} = 3.5$) (Extended Data Fig. 7a). The identity of these dimensions varies across niches reflecting adaptations associated with contrasting modes of life (Extended Data Fig. 8). Taking all trophic niches together, an integrated niche space is minimally described by a 4-dimensional morphospace ($D_{\mathrm{Total}} = 4.4$). Decreasing dimensionality from four to one dimension results in an almost linear decline in the ability to predict trophic niches, while increasing dimensionality from four dimensions upwards only results in marginal improvement in niche predictability (Extended Data Fig. 7a). Similar estimates of trophic niche dimensionality were obtained regardless of the method used to match traits and ecology (see Methods) and whether or not we accounted for the phylogenetic non-independence of species (Extended Data Fig. 7b). These consistent results suggest that trophic niche space is inherently, yet nonetheless moderately, multidimensional. On the one hand, a four-dimensional hypervolume challenges the view[23,24] that animal trophic niches can be collapsed along an axis of body size, or indeed any single trait dimension. On the other hand, the level of dimensionality seems remarkably limited given the scale of ecomorphological variation encompassed by the entire avian radiation.

It seems plausible that our use of simple linear measurements has led to an underestimation of niche dimensionality and that additional or more sophisticated body shape measurements—such as beak curvature[43]—may reveal further axes of ecological variation. However, the increment in niche-related information is probably minor at the scale of our analyses, particularly since simulations suggest that our estimate of dimensionality is robust to the addition of numerous alternative traits (see Methods). Limited dimensionality could also reflect the coarseness of our niche classification, so we reran the random forest models based on niches subdivided into more precise categories relating to foraging behaviours and substrates (Supplementary Table 4). We found that more trait dimensions are indeed required to predict this finer-grained classification system ($\bar{D} = 4.1$, $D_{\mathrm{Total}} = 5.6$; Extended Data Fig. 7c), with the trait axes defining trophic niches forming a nested subset of those defining foraging niches (Extended Data Fig. 8; see Methods). However, the increase in niche dimensionality is minor, suggesting a hierarchical structure to niche space whereby the same dimensions are repeatedly partitioned across multiple ecological scales[45]. While these results provide compelling evidence that multitrophic niche space is predictably organized along a limited number of fundamental trait dimensions, they tell us little about how this correspondence between form and function has arisen.

Evolution of form–function relationships. One explanation for the apparent matching between form and function is that closely

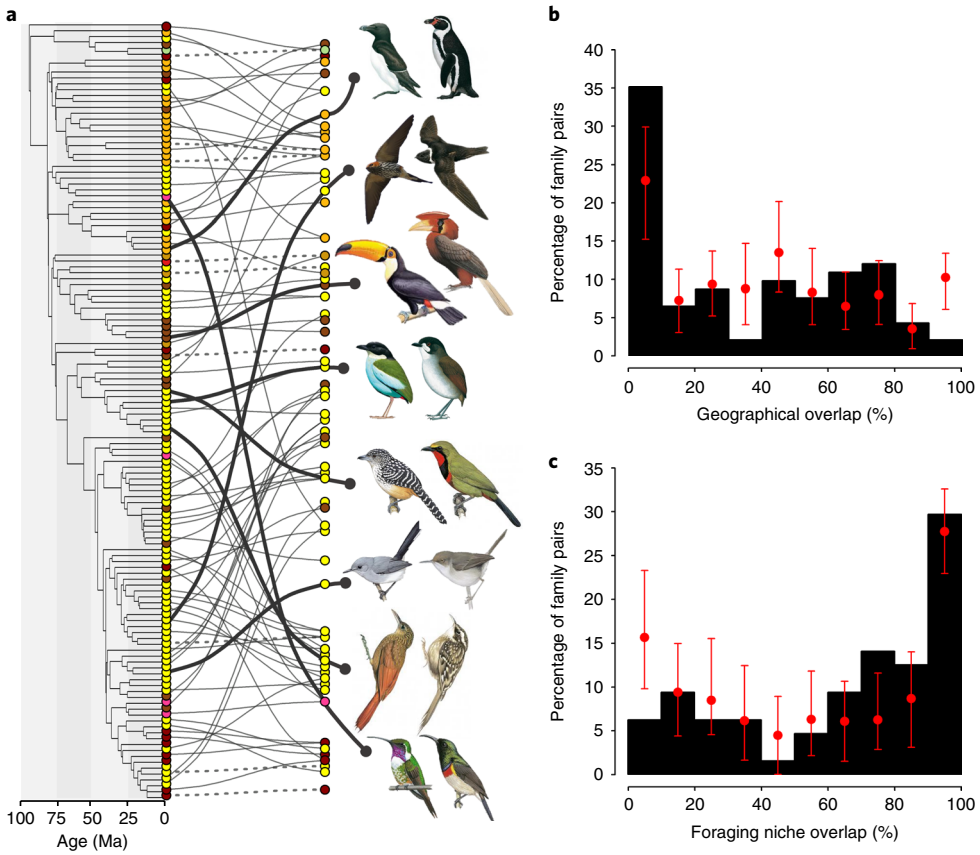

Fig. 4 | Scale and context of macroevolutionary convergence in birds. a, The lines connect phenotypically matched families ($n = 91$ pairs) spanning the avian evolutionary tree. Exemplars are highlighted with bold lines, sister clades with dashed lines. Tree tips are coloured according to the predominant trophic niche (see Fig. 3). **b**,**c**, Matched family pairs are not randomly distributed in relation to geographical ($n = 91$ pairs) (**b**) and foraging niche overlap ($n = 64$ pairs) (**c**), with most cases having disjunct geographical distributions and similar foraging niches. The red points and whiskers show the expectation (median and 95% confidence interval) under a null model of trait evolution (see Methods). Bird images reproduced with permission from HBW, Lynx Edicions.

related species tend to occupy the same niche and have similar traits simply because of shared ancestry[46]. Alternatively, each trophic niche may have evolved multiple times, with the strong match between form and function arising from repeated phenotypic convergence towards the same adaptive optima[26,47]. The extent to which phylogenetic history or adaptive evolution shape current ecological diversity is unclear. To address this, we compared the strength of the relationship observed between form and trophic function to that expected under an evolutionary null model where similarity in species traits depends on the time elapsed since lineages diverged as well as variation in the rate of stochastic trait evolution (see Methods). We found that this model can account for a substantial fraction of the match between form and trophic niches (Expected accuracy = 65% (95% confidence interval: 60–70%)) but is insufficient to explain the striking predictability of avian ecological functions (observed accuracy = 85%). Although each trophic niche is populated by multiple distantly related clades (Extended Data Fig. 9a), these lineages are far more tightly packed in morphospace (Fig. 3) than would be expected based on their evolutionary relatedness (Extended Data Fig. 9b). Thus, while our results highlight the major imprint of phylogenetic history on the structuring of avian trophic diversity, they also suggest that the correspondence between form and function requires an adaptive explanation.

To explore these evolutionary patterns in more detail, we identified 91 pairs of avian families with the most similar traits within each trophic niche (see Methods). We found that some (10%) morphologically matched families are sister clades wherein phenotypic similarity can be explained by shared ancestral traits (Fig. 4a). However, most pairings represent much more ancient divergence events (median divergence time = 55 (interquartile range: 39–75) million years (Ma) versus 28 (interquartile range: 21–51) Ma for sister clades), suggesting that trait similarity has resulted from convergent evolution (Fig. 4a).

Classifying phenotypic convergence events by spatial context revealed that such cases tend to occur in pairs of clades with non-overlapping geographical distributions more often than expected by chance (Fig. 4b; see Methods). We also assessed whether similarity in foraging niches predicted evolutionary convergence events in the two most heterogeneous trophic groups (aquatic predators and terrestrial invertivores). In these diverse niches, we found that convergence occurred primarily among pairs of families using the same foraging techniques, again rejecting a null model of random convergence (Fig. 4c). A key role for both geographical isolation and ecological similarity is consistent with the view that macroevolutionary convergence is driven by adaptation to vacant ecological niches[47]. Thus, the Neotropical region is home to arboreal frugivorous toucans (Ramphastidae) and ground-dwelling invertivorous antpittas (Grallariidae), which are replaced in the palaeotropics by hornbills (Bucerotidae; Fig. 5a) and pittas (Pittidae; Fig. 5b), respectively. A minority of families, such as swallows (Hirundinidae) and swifts (Apodidae), appear to have converged despite broad spatial overlap (Fig. 5c), although it is plausible that the early stages of convergence occurred in geographical isolation.

By tracing evolutionary trajectories through morphospace, we can visualize the probable history of convergence events according

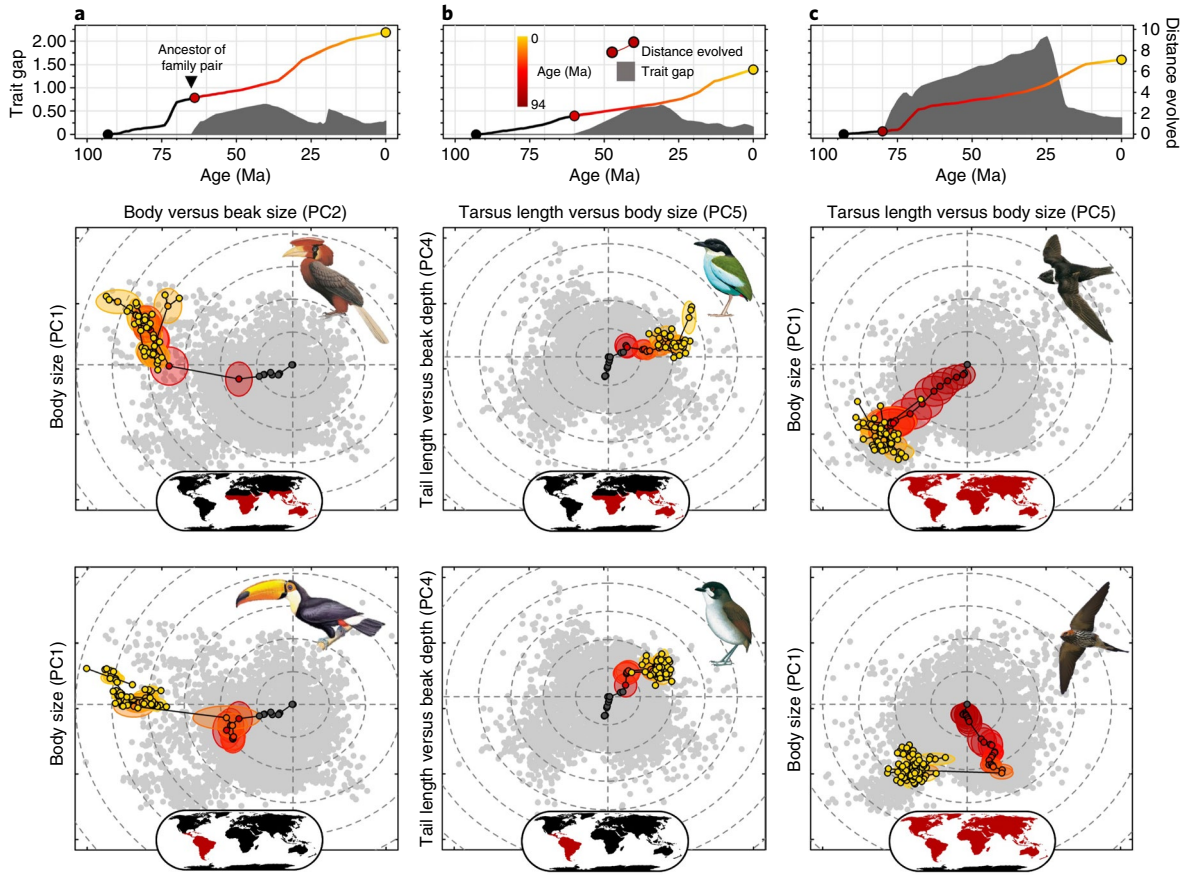

Fig. 5 | Convergent evolutionary trajectories through avian morphospace. a–c, To illustrate the probable history of convergence events, data from ancestral trait reconstructions are shown for three exemplar pairs of convergent avian families (**a**, top, Bucerotidae; bottom, Ramphastidae; **b**, top, Pittidae; bottom, Grallaridae; **c**, top, Apodidae; bottom, Hirundinidae). The uppermost panels show the cumulative phenotypic distance travelled by each family pair through morphospace and the corresponding phenotypic gap between families. Phylomorphospace plots (lower panels) show the position of ancestral nodes within each clade (the transition from yellow to red indicates increasing time before the present, Ma) and before divergence of the family pair (grey). The size of the discs around the nodes indicates uncertainty in trait reconstruction. Nodes leading to other lineages are not shown. Maps show global distribution of each family in relation to biogeographical realms (see Fig. 6). Bird images reproduced with permission from HBW, Lynx Edicions.

to a global phylogenetic tree[41]. These reconstructions show that, within matched family pairs, each clade has on average evolved a distance equivalent to one-third the span of total avian morphospace before arriving at its current position (Fig. 5a–c and Extended Data Fig. 10). In some cases (illustrated in Fig. 5a), family pairs have followed largely parallel trajectories, while in others (Fig. 5b,c) convergence has occurred from different points in morphospace, such that the current gap between families is substantially narrower than it was in the past.

A corollary of widespread convergent ecological adaptation to geographically segregated vacant niche space is that species occupying a given niche will cluster together in morphospace regardless of their geographical origins. To reveal this global mapping of form to function, we partitioned the avian hypervolume into biogeographical realms (see Methods). We found that each trophic niche has the same morphological signature worldwide, highlighting the repeatability of convergence events across multiple evolutionary arenas (Fig. 6).

Conclusions

The connection between avian morphospace and trophic niches provides compelling evidence of widespread deterministic convergence in a diverse multitrophic assemblage[27]. Our analyses reveal that the predictable patterns of niche filling observed among individual lineages[26,48], or in more localized settings[47,49], are part of a grander evolutionary dynamic operating across entire classes of organisms at a global scale. This pervasive convergent evolution of morphological traits overrides the imprint of phylogenetic history in structuring avian niche space, reducing the power of phylogenetic biodiversity metrics to predict ecological function[50] unless combined with other information about traits. We have demonstrated that a minimum of four independent morphological trait axes are required to predict variation in avian trophic niches, calling into question the validity of trait-based macroecological analyses that assess functional diversity on the basis of fewer morphological trait dimensions (for example, body mass). We also show that continuous morphological variables can predict much subtler fine-scale variation in dietary and behavioural niches than can be achieved using standard niche categories (for example, diet).

More generally, these findings have relevance to multiple environmental research programmes and policy frameworks, many of which have taken on increased urgency in light of rapid declines in animal diversity and abundance[3,4]. The avian trait space presented in this study, which is based on the most complete sample of morphological variation for any major taxon, provides a highly resolved template linking species traits to ecological function. Trait variation within any avian trophic guild, or clade, or indeed any historical, contemporary or predicted future bird community, can be mapped onto this template and interpreted in the context of

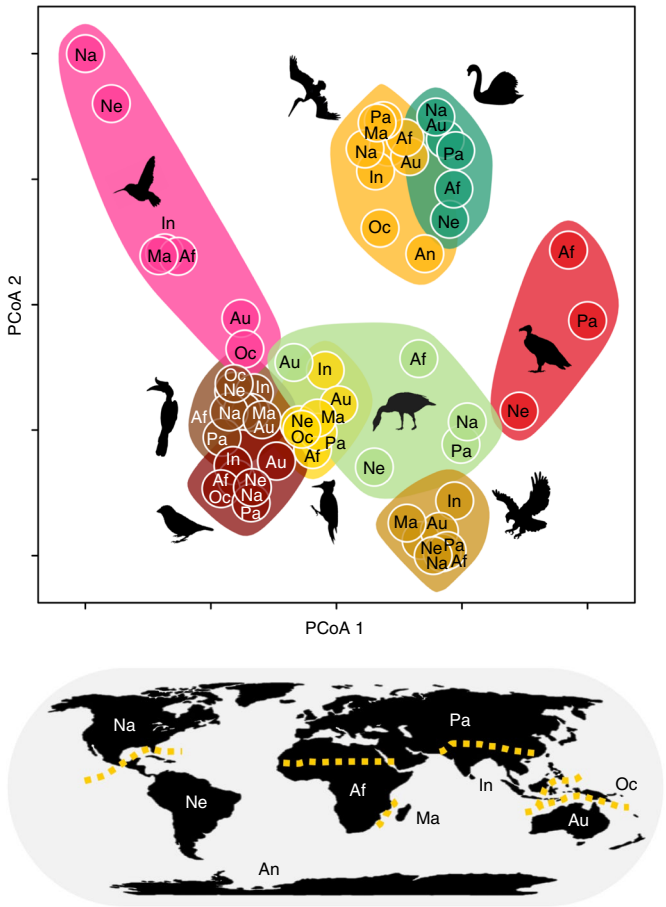

Fig. 6 | The global mapping of form to function across birds. Clustered points along each principal coordinate axis (PCoA) show the relative morphological similarity between trophic niches from different ecological theatres (biogeographical realms) based on the average pairwise distance between species ($n = 9{,}963$ species) in nine-dimensional morphospace (see Methods). Individual trophic niches are omitted where they are absent or rare (<6 species) within particular biogeographic realms (Na, Nearctic; Ne, Neotropic; Pa, Palaearctic; Af, Afrotropic; Ma, Madagascar; In, Indo-Malaya; Oc, Oceania; Au, Australasia; An, Antarctic). Bird images reproduced with permission from HBW, Lynx Edicions.

regional or global patterns. In practical terms, this resource paves the way to a new generation of functional and behavioural diversity indicators for use in setting and measuring progress towards international conservation targets, understanding functional effects of extinction[51] and evaluating how animal communities assemble and respond to change[16,29,52].

Methods

Morphological trait data. We assembled a dataset of morphometric measurements from 52,870 live-caught individuals and preserved museum skins; 2,288 specimens were from existing published datasets[53,54]. In total, our dataset represents 9,963 of the 9,993 extant species (99.7%) recognized in the global avian taxonomy used by Jetz et al.[41]. For each individual, we measured 8 traits (generally to the nearest 0.1 mm): beak length from tip to skull along the culmen; beak length to the nares; beak width at the nares; beak depth at the nares; tarsus length; wing length; first secondary length; and tail length (see Extended Data Fig. 1 and Supplementary Table 1 for further descriptions). We obtained measurements from at least 4 adult individuals from each species where possible (2 from each sex; mean total = 5.3 individuals). Sampling was conducted by 93 researchers across 65 museum collections worldwide using a standard protocol (see Supplementary Information). To assess repeatability, we compiled measurements by different researchers on the same specimens ($n = 2{,}752$ individuals of 2,523 species). Repeated measures were highly concordant since measurer identity accounted for only 0.74% of total trait variance in this dataset (Extended Data Fig. 2; see Supplementary Information for details). We extracted estimates of mean species body mass (g) from Wilman et al.[40], largely based on the compilation by Dunning[55]. To match the species-level resolution of our ecological niche data (see Ecological niche data section for details), we calculated mean trait values for each species. This is justifiable because most of the variance in trait values occurs between (98.25%) rather than within (1.75%) species (Supplementary Table 1; see Supplementary Information for details). We performed a principal components analysis (PCA) on the log-transformed mean species trait values. We centred and rescaled each phenotypic trait to unit variance before performing two separate PCAs using (1) the four beak measurements (beak length at the nares and culmen, beak width and depth at the nares) and (2) all nine phenotypic traits (Extended Data Fig. 3). We visualized the distribution of species throughout nine-dimensional morphospace by calculating the density of species within concentric shells with a width of one morphological unit (Extended Data Fig. 4).

Ecological niche data. For each species, we scored the proportion of its diet obtained from three trophic levels (primary consumer; secondary/tertiary consumer; scavenger) and nine trophic niches (aquatic herbivore; terrestrial herbivore; nectarivore; granivore; frugivore; aquatic predator; invertivore; vertivore; scavenger) encompassing the major resource types used by birds (Extended Data Fig. 5a). Our scoring of species diets is primarily based on data from Wilman et al.[40], extensively updated and reorganized based on recent literature. For instance, we classified species eating any kind of aquatic prey as aquatic predators, whereas in Wilman et al.[40] species feeding on aquatic and terrestrial invertebrates were grouped together (for example, flamingos with warblers). Based on these dietary scores we assigned species to the trophic level from which they obtained at least 70% of their resources, with species using multiple trophic levels in relatively equal proportions classified as 'omnivores'[56]. Similarly, we assigned species to the trophic niche from which they obtained at least 60% of their resources. (This lower threshold was chosen due to the larger number of trophic niche categories[56].) Species using multiple niches, within or across trophic levels, in relatively equal proportions were classified as 'trophic generalists'. Although not all omnivores are trophic generalists, and vice versa, there is nonetheless broad overlap; for simplicity, we use the term 'omnivore' when referring to both categories together.

Following the standardized protocol outlined in Wilman et al.[40], we used the extensive literature on avian feeding ecology and behaviour (for example, del Hoyo et al.[57]) to quantify for each species the relative use of 31 different foraging niches (scored in 10% intervals), describing different combinations of diet, foraging manoeuvre and substrate (Extended Data Fig. 5b,c). These foraging niches expand on previous guild classifications[31,32,34,58–61] to reflect the wider taxonomic and ecological scope of our analysis. Based on these scores, we assigned each species occupying a specialist trophic niche (that is, excluding omnivores) to the foraging strategy by which it accessed at least 60% of its dominant resource type. Two foraging niches (ground and arboreal gleaning vertivores) were each represented by only six species and so were excluded. Species using multiple foraging strategies in relatively equal proportions were classified as 'foraging generalists', thus providing a total of 30 foraging niches used in our analysis. Detailed descriptions of each foraging niche are provided in Supplementary Table 4. Species morphological principal component scores and ecological niche assignments are provided in Supplementary Dataset 1.

Phylogenetic data. To explore the evolutionary basis of form–function relationships, we used the time-calibrated molecular phylogeny of Jetz et al.[41] using the Hackett et al.[62] backbone. To ensure reliable estimates of evolutionary parameters, we restricted our phylogenetic analyses to the 6,666 species with morphological data and for which branch lengths were estimated on the basis of genetic data. Because the evolutionary models we use are computationally expensive to fit to the entire avian phylogeny, we based our analysis on the maximum clade credibility tree generated from across 1,000 trees sampled at random from the posterior distribution using TREEANNOTATOR, which is included in BEAST v.1.6.1 (ref. [63]).

Geographical data. Range maps of species breeding distributions were obtained from BirdLife International (http://www.birdlife.org/datazone/home). Owing to the taxonomic lumping or splitting of various lineages, there are differences in the species classification used by the International Union for Conservation of Nature (IUCN) and Jetz et al.[41]. We aligned the IUCN dataset with that of Jetz et al.[41] by editing species range maps in ArcMap v.0.3 (ref. [64]) based on published information on the geographical ranges of relevant taxa[57]. Species ranges were then extracted onto an equal area grid (Behrmann projection) with a resolution of 110 km (≈1° at the equator).

Quantifying the match between traits and niches. We tested whether species ecological niches can be predicted on the basis of species traits using random forest models[65] implemented using the R v.3.5.2[66] package randomForest v.4.6-14[67]. This method is suitable for matching traits to ecology because it makes minimal assumptions about the shapes of species niches and can accommodate interactions across multiple trait axes. Random forest models use an ensemble of decision trees

to partition feature space (that is, morphospace) into a set of non-overlapping rectangular hypervolumes within which impurity in ecological niches is minimized (Supplementary Fig. 1). Thus, each internal node in a tree corresponds to a split along one randomly selected dimension of morphospace, with each terminal node corresponding to a unique rectangular hypervolume. Each decision tree in the random forest provides a 'vote' on the identity of a species' ecological niche based on its position in morphospace. We used the majority vote across trees to predict the ecological niche of species and then calculated the proportion of species correctly assigned to each niche. Throughout, we report overall model predictive performance as the mean classification accuracy across ecological niches. Model parameters, including the number of trees ($n=500$) and the number of random traits to sample at each node ($n=2$), were selected based on initial sensitivity tests.

Because species are highly unevenly distributed across ecological niches, we randomly upsampled or downsampled each niche to an equivalent number of species before fitting the models ($n=5{,}000$, 2,000 and 1,000 species for trophic levels, trophic niches and foraging niches, respectively). To provide unbiased estimates of predictive performance, we used fivefold cross-validation. We randomly split our data into five equally sized sets, maintaining the same relative frequency of each ecological niche within each set. We trained a model on 80% of the data ('training set') and used this to predict species niches in the remaining 20% of the data ('test set'), repeating this 5 times, once for each partition. To account for stochasticity in model fit arising from the random partitioning of the dataset during cross-validation, we fitted 11 replicate models and used the modal prediction for each species. We compared the predictive performance of random forest models including: (1) only body mass; (2) body mass and principal component scores based on all beak measurements (length, width and depth); and (3) principal component scores based on all nine phenotypic traits.

Sensitivity tests of trait niche matching. While the random forest model detects a strong statistical match between traits and ecological niches (Fig. 2), it is possible that this accuracy is only achieved through a highly complex mapping of form to function. For example, each niche could consist of multiple, widely scattered clusters in morphospace representing a series of unique evolutionary radiations. If one member of each cluster is included in the training dataset, we may infer a high statistical predictability of trophic niches, despite the link between morphology and ecology being unpredictable (that is, not repeatable) in an evolutionary sense[26]. We examined this by (1) refitting a random forest model constraining the number of terminal nodes permitted in each tree and (2) repeating our analysis using linear (LDA) and mixture discriminant analysis (MDA). Discriminant analysis is widely used to match variation in ecology and morphology based on restrictive assumptions about the shape of ecological niches. Unlike our random forest model, LDA assumes that each niche corresponds to a single multivariate, normally distributed morphological cluster, with equal variance across niches. MDA relaxes these assumptions by allowing each niche to be modelled by a Gaussian distribution of subclasses, with an equal covariance structure across subclasses.

First, we found that even when random forest tree size is strongly constrained (for example, $n=20$ terminal nodes), predictive accuracy remains high, indicating that each trophic niche can be well described by 1 or a few rectangular hypervolumes (Supplementary Fig. 2). Second, despite restrictive assumptions, the LDA and MDA predicted specialist trophic niches with 71 and 80% accuracy, respectively (Extended Data Fig. 6). Thus, additional analyses support high predictability of ecological niches, indicating that the strong match between traits and ecology does not arise from overfitting of the random forest model and instead reflects a relatively simple one-to-one mapping of morphology to ecological niches.

Simulations show that, depending on the shape and arrangement of ecological niches in morphospace, MDA and LDA may underestimate the true match between traits and ecological niches (Supplementary Fig. 3). Specifically, when niches occur as disjunct clusters in morphospace, as observed in some smaller species radiations (for example, *Anolis* lizards[47]), then LDA and MDA accurately predict niche identity (Supplementary Fig. 3a,b). However, when niches have irregular shapes that closely abut in morphospace, as in our empirical dataset (Fig. 3), species along the boundaries of each niche may be misclassified leading to a lower predictive accuracy (LDA = 84%, MDA = 95%) (Supplementary Fig. 3c,d). In contrast, a random forest model can readily incorporate close nonlinear relationships, providing a more robust estimate of the match between morphology and ecology. Therefore, we focus our analysis on the results from the random forest model.

Phylogenetic null model of trait niche relationships. The predictable relationship between traits and ecological niches may simply reflect shared phylogenetic ancestry. We assessed this possibility by comparing the empirical estimates of niche predictability to those expected under an evolutionary null model. Keeping the trophic niche of each species fixed, we simulated morphological trait values according to a Brownian motion model of trait evolution applied to the avian phylogenetic tree (see the Phylogenetic models of Brownian trait evolution section for details)[68]. This null model allowed us to quantify the similarity in species traits expected due to phylogenetic relatedness in the absence of ecological adaptation. We fitted a random forest model to each of 100 replicate simulated trait distributions to calculate the expected predictability of overall niche space and each individual trophic niche (Supplementary Fig. 4). We repeated this analysis using MDA and LDA as alternative methods to match traits to niches and obtained similar results (Supplementary Fig. 4). As a further test, we assessed whether species sharing the same trophic niche are more densely packed in trait space than expected under the evolutionary null model by comparing the mean pairwise Euclidean trait distance between species within each trophic niche to that expected across 1,000 simulations of the null model (Extended Data Fig. 9).

Phylogenetic models of Brownian trait evolution. We parameterized the null model of Brownian trait evolution according to the empirical rates of trait evolution estimated across the avian phylogenetic tree using BAMM v.2.5.0[69,70]. This modelling framework uses reversible-jump Markov chain Monte Carlo to fit a set of distinct macroevolutionary regimes across the phylogenetic tree, the number, location and parameters of which are estimated from the data. Each regime may be characterized by a different rate and dynamic of trait evolution, including either increasing or decreasing rates through time. Unlike many studies, we are not specifically interested in these estimated parameters per se; instead, we simply use them to parameterize our null model simulations to account for the potentially complex dynamics of avian phenotypic evolution.

We fitted this model separately to each of our nine principal component trait axes to estimate marginal densities of phenotypic rates on each branch of the avian phylogeny. Sensible priors on rate parameters were assigned using the settBAMMpriors functions. We ran the Markov chain Monte Carlo simulation for 600 million generations, sampling the parameters every 80,000 generations. We discarded the first 10% of samples as burn-in and assessed convergence by calculating the effective sample size of the model log-likelihood and the estimated number of macroevolutionary regime shifts. The effective sample size for each trait was consistently above the recommended value of 200. We used the mean marginal rate configuration across the phylogeny to parameterize the simulations.

Quantifying the dimensionality of trophic niche space. To quantify the dimensionality of trophic niche space, we fitted random forest models to morphospaces consisting of 1–9 trait dimensions, exploring all possible combinations of principal component trait axes ($n=511$ trait combinations for 9 traits; Extended Data Fig. 7a). For each level of dimensionality, we identified the combination of trait axes that provided the highest mean niche predictability (Extended Data Fig. 8a,b). In one dimension, PC1 is the optimal trait axis. However, in higher dimensions the identity of the optimal trait axes does not simply correspond to their relative contribution to total phenotypic variance. For instance, in three dimensions, trophic niche space is best described by PC1, PC3 and PC4 rather than PC2 (Extended Data Fig. 8a). In general, trait axes accounting for only a minor fraction to the total phenotypic variance contribute disproportionately to defining ecological niche space.

Using the maximum predictive accuracy at each level of morphospace dimensionality, we calculated the dimensionality of trophic niche space (D_{Total}) according to Levene's index[71]:

$$D_{\mathrm{Total}} = \frac{1}{\sum p_i^2}$$

where p_i is the proportion of the maximum predictive accuracy (across all trait combinations) accounted for by dimension i. We applied the same approach to calculate the dimensionality of each individual trophic niche and also foraging niche space.

The core trait dimensions identified using these estimates of dimensionality varied across niches in ecologically informative ways (Extended Data Fig. 8c,d). For instance, it makes sense that PC7 forms one of three core axes of the granivore (seed-eating) niche because it describes the ratio of beak depth to width, with higher values corresponding to a stronger bite force and ability to crush seeds[39]. Similarly, one of three core axes of the aquatic predator niche is PC8, a correlate of wing pointedness, with higher values corresponding to greater soaring ability and flight efficiency[72].

Sensitivity tests of niche dimensionality. To assess the robustness of our estimates of niche dimensionality D, we performed multiple sensitivity tests. First, we repeated our analysis using synthetic morphological axes generated from a phylogenetic PCA that accounts for the non-independence of species[73]. Estimates of niche dimensionality ($D_{\mathrm{Total}}=4.4$) and predictive accuracy (81%) obtained using this method were very similar to those based on phylogenetically uncorrected principal component axes (Extended Data Fig. 7a,b). Second, rather than a random forest model we used LDA and MDA to predict trophic niches. Estimates of trophic niche dimensionality (D_{Total}) vary from $D_{\mathrm{Total}}=3.3$ for MDA to $D_{\mathrm{Total}}=6$ for LDA, with a random forest model providing an intermediate estimate of $D_{\mathrm{Total}}=4.4$ (Supplementary Fig. 5). At the scale of foraging niches, estimates of dimensionality were more constrained varying from $D_{\mathrm{Total}}=5.6$ (random forest and MDA) to $D_{\mathrm{Total}}=6$ (LDA) (Supplementary Fig. 5). Thus, all models agree that (1) trophic niche space is minimally described by at least four complete trait dimensions and that (2) when niches are resolved at a much finer scale (that is, foraging behaviours and substrates), dimensionality increases only marginally, with niche space described with six or fewer trait dimensions. Given the higher predictive accuracy of the random forest model and the known sensitivity of MDA and LDA to niche shape, we consider the random forest estimates to be the most robust (see Sensitivity tests of trait niche matching section and Supplementary Fig. 3).

Our trait sampling generates imperfect predictions of trophic niches, suggesting that additional trait axes may be required to fully describe niche space, leading to potentially higher estimates of dimensionality. To explore this possibility, we simulated how total niche dimensionality (D_{Total}) changes when the remaining variation in niches left unexplained by our nine-dimensional morphospace is equitably divided among an additional number of hypothetical trait dimensions. Simulations show that even with the addition of many hypothetical trait axes (for example, $n = 100$ trait dimensions), our estimate of trophic niche dimensionality increases only marginally ($D_{Total} = 6.1$ versus 4.4; Supplementary Fig. 6a). D_{Total} is robust to this proliferation of trait dimensions because so much variation in trophic niches is explained by our existing nine-dimensional morphospace (Extended Data Fig. 7a). Estimates of foraging niche dimensionality are potentially more sensitive to the inclusion of additional trait axes, with our simulations suggesting an upper bound of $D_{Total} < 11$ (Supplementary Fig. 6b). However, we note that these simulations probably overestimate the potential increase in dimensionality from measuring additional traits. For instance, if some variation in ecology occurs independently of traits or if there are differences in the amount of ecological variation explained by hypothetical trait dimensions, this leads to substantially smaller increases in D_{Total} (Supplementary Fig. 6b). Thus, our simulations should be viewed as providing an upper bound on niche dimensionality.

Identifying phenotypically matched families. To identify clades with similar ecologies that are most similar in their functional traits, we assigned avian families to one of three functional groups: (1) primary consumers; (2) terrestrial secondary/tertiary consumers; and (3) aquatic secondary/tertiary consumers. We restricted the analysis to families containing more than 5 species with both genetic and morphological data ($n = 132$). Because relatively few large families were aquatic primary consumers or scavengers, these groups were lumped with terrestrial primary consumers and terrestrial secondary/tertiary consumers, respectively. Within each of these functional groups, we identified phenotypically matched pairs of families by fitting a random forest model predicting family identity on the basis of morphological traits and then calculating the mean species proximity scores for each pairwise combination of clades. These scores indicate the proportion of times a species in a clade is assigned to the same rectangular hypervolume as a species from another clade. This metric of proximity has an advantage over standard distance-based measures (for example, Euclidean distances) because it does not require any assumptions regarding the relative importance of different trait axes in discriminating between families. Instead, this information is learned from the data. In total, we identified 91 unique family pairs (41 reciprocally matched pairs were only counted once in the analysis) (Supplementary Dataset 2).

Reconstructions of ancestral traits. To visualize how matched family pairs have evolved similar trait values, we used the branch- and trait-specific rate estimates obtained from our BAMM analysis along with the fastAnc function in the R package phytools[74] to reconstruct trait values (and 95% confidence intervals) at each node in the phylogenetic tree as well at 1-Ma time intervals along each branch[75]. For each time step, we quantified the mean position of each family along each trait axis, and summed the Euclidean distance between these successive time points to estimate the total distance evolved across morphospace by each family since they diverged[76]. To visualize the evolutionary trajectories of selected families through morphospace (Fig. 4b–d), we also calculated the trait gap (that is, 5% quantile of minimum pairwise distances) between each family at each 1-Ma time interval[76].

Different family pairs occupy different trophic and foraging niches and these niches are defined by different sets of traits (Extended Data Fig. 8). Therefore, when calculating phenotypic distance metrics, we selected the two trait axes that best describe the niche of each family pair (Supplementary Dataset 2). These trait axes were identified using the mean ranking of variable importance scores across the two families from the random forest model. To compare the distance metrics based on different combinations of trait axes, we rescaled current and ancestral species trait values to unit variance before calculating phenotypic distances. We express these distances as a proportion of the total span of avian morphospace, calculated as the diameter of a circle centred on the centroid of morphospace and containing 95% of species (Extended Data Fig. 10).

Ecology and geographical distribution of phenotypically matched clades. To explore the geographical and ecological context of convergence, we quantified the spatial overlap and similarity in foraging behaviour of families within matched pairs (Supplementary Dataset 2). Spatial overlap between families ($n = 91$ pairs) was quantified using the summed proportion of each species geographical range occurring in each of 9 biogeographical realms[77]. The foraging niche overlap between families of aquatic predators and invertivores ($n = 64$ pairs) was quantified using the summed proportional use of each foraging niche. Spatial and foraging overlap were scored using Schoener's D statistic (denoted by the symbol S to distinguish it from our dimensionality metric):

$$S(p_X, p_Y) = 1 - \frac{1}{2}\sum_i |p_{X,i} - p_{Y,i}|$$

where $p_{X,i}$ (or $p_{Y,i}$) is the proportional use of region/niche i by species x (or y). Values of S vary from 0 (no overlap) to 1 (complete overlap) and were multiplied by 100 to report the overlap scores for each family pair from 0 to 100% (in 10% intervals).

If families are restricted to single biogeographical realms or foraging niches, then many family pairs would be expected to show little spatial or ecological overlap simply by chance. Therefore, we compared the observed frequency of spatial and foraging overlap to that expected under 100 replicate simulations of our phylogenetic null model, where matched family pairs are generated through a process of complex Brownian trait evolution (see the Phylogenetic null model of trait niche relationships section for details).

To visualize the effects of these non-random evolutionary dynamics, we generated a matrix of pairwise trait distances between the species in the full nine-dimensional morphospace. We calculated the mean distance between species in each combination of trophic niche and biogeographical realm and used non-metric multidimensional scaling to translate this distance matrix onto two orthogonal principal coordinate axes.

Reporting Summary. Further information on research design is available in the Nature Research Reporting Summary linked to this article.

Data availability

All geographical and phylogenetic data are publicly available from www.birdlife.org and www.birdtree.org, respectively. Morphological data and ecological niche assignments are provided in Supplementary Dataset 1.

Code availability

The code to conduct the analyses is available on request from the authors.

Received: 21 June 2019; Accepted: 20 November 2019;
Published online: 13 January 2020

References

1. Elton, C. S. *Animal Ecology* (Macmillan, 1927).
2. Butterfield, N. J. Animals and the invention of the Phanerozoic Earth system. *Trends Ecol. Evol.* **26**, 81–87 (2011).
3. Estes, J. A. et al. Trophic downgrading of planet Earth. *Science* **333**, 301–306 (2011).
4. Dirzo, R. et al. Defaunation in the Anthropocene. *Science* **345**, 401–406 (2014).
5. Díaz, S. et al. The global spectrum of plant form and function. *Nature* **529**, 167–171 (2016).
6. Lauder, G. V. in *Functional Morphology in Vertebrate Paleontology* (ed. Thomason, J. J.) 1–18 (Cambridge Univ. Press, 1995).
7. Carroll, S. Chance and necessity: the evolution of morphological complexity and diversity. *Nature* **409**, 1102–1109 (2001).
8. Wainwright, P. C. Functional versus morphological diversity in macroevolution. *Annu. Rev. Ecol. Evol. Syst.* **38**, 381–401 (2007).
9. Losos, J. B. Convergence, adaptation, and constraint. *Evolution* **65**, 1827–1840 (2011).
10. Bascompte, J. & Jordano, P. Plant-animal mutualistic networks: the architecture of biodiversity. *Annu. Rev. Ecol. Evol. Syst.* **38**, 567–593 (2007).
11. Peck, A. L. *Aristotle: History of Animals* (Harvard Univ. Press, 1970).
12. Cernansky, R. Biodiversity moves beyond counting species. *Nature* **546**, 22–24 (2017).
13. Kraft, N. J. B., Godoy, O. & Levine, J. M. Plant functional traits and the multidimensional nature of species coexistence. *Proc. Natl Acad. Sci. USA* **112**, 797–802 (2015).
14. Larcombe, M. J., Jordan, G. J., Bryant, D. & Higgins, S. I. The dimensionality of niche space allows bounded and unbounded processes to jointly influence diversification. *Nat. Commun.* **9**, 4258 (2018).
15. Diaz, S. & Cabido, M. Vive la différence: plant functional diversity matters to ecosystem processes. *Trends Ecol. Evol.* **16**, 646–655 (2001).
16. McGill, B. J., Enquist, B. J., Weiher, E. & Westoby, M. Rebuilding community ecology from functional traits. *Trends Ecol. Evol.* **21**, 178–185 (2006).
17. Lavorel, S. & Garnier, E. Predicting changes in community composition and ecosystem functioning from plant traits: revisiting the Holy Grail. *Funct. Ecol.* **16**, 545–556 (2002).
18. Purves, D. et al. Ecosystems: time to model all life on earth. *Nature* **493**, 295–297 (2013).
19. Didham, R. K., Leather, S. R. & Basset, Y. Circle the bandwagons: challenges mount against the theoretical foundations of applied functional trait and ecosystem service research. *Insect Conserv. Divers.* **9**, 1–3 (2016).
20. Gravel, D., Albouy, C. & Thuiller, W. The meaning of functional trait composition of food webs for ecosystem functioning. *Philos. Trans. R. Soc. Lond. B* **371**, 20150268 (2016).
21. Hutchinson, G. E. Concluding remarks. *Cold Spring Harb. Symp. Quant. Biol.* **22**, 415–427 (1957).

22. Schoener, T. W. Resource partitioning in ecological communities. *Science* **185**, 27–39 (1974).
23. Cohen, J. E. *Food Webs and Niche Space* (Princeton Univ. Press, 1978).
24. Williams, R. J. & Martinez, N. D. Simple rules yield complex food webs. *Nature* **404**, 180–183 (2000).
25. Shoval, O. et al. Evolutionary trade-offs, pareto optimality, and the geometry of phenotype space. *Science* **336**, 1157–1160 (2012).
26. Blount, Z. D., Lenski, R. E. & Losos, J. B. Contingency and determinism in evolution: replaying life's tape. *Science* **362**, eaam5979 (2018).
27. Winemiller, K. O., Fitzgerald, D. B., Bower, L. M. & Pianka, E. R. Functional traits, convergent evolution, and periodic tables of niches. *Ecol. Lett.* **18**, 737–751 (2015).
28. Laughlin, D. C. The intrinsic dimensionality of plant traits and its relevance to community assembly. *J. Ecol.* **102**, 186–193 (2014).
29. Petchey, O. L. & Gaston, K. J. Functional diversity (FD), species richness and community composition. *Ecol. Lett.* **5**, 402–411 (2002).
30. Eklöf, A. et al. The dimensionality of ecological networks. *Ecol. Lett.* **16**, 577–583 (2013).
31. Miles, D. B. & Ricklefs, R. E. The correlation between ecology and morphology in deciduous forest passerine birds. *Ecology* **65**, 1629–1640 (1984).
32. Pigot, A. L., Trisos, C. H. & Tobias, J. A. Functional traits reveal the expansion and packing of ecological niche space underlying an elevational diversity gradient in passerine birds. *Proc. Biol. Sci.* **283**, 20152013 (2016).
33. Bright, J. A., Marugán-Lobón, J., Cobb, S. N. & Rayfield, E. J. The shapes of bird beaks are highly controlled by nondietary factors. *Proc. Natl Acad. Sci. USA* **113**, 5352–5357 (2016).
34. Miller, E. T., Wagner, S. K., Harmon, L. J. & Ricklefs, R. E. Radiating despite a lack of character: ecological divergence among closely related, morphologically similar honeyeaters (Aves: Meliphagidae) co-occurring in arid Australian environments. *Am. Nat.* **189**, E14–E30 (2017).
35. Felice, R. N., Tobias, J. A., Pigot, A. L. & Goswami, A. Dietary niche and the evolution of cranial morphology in birds. *Proc. Biol. Sci.* **286**, 20182677 (2019).
36. Navalón, G., Bright, J. A., Marugán-Lobón, J. & Rayfield, E. J. The evolutionary relationship among beak shape, mechanical advantage, and feeding ecology in modern birds. *Evolution* **73**, 422–435 (2019).
37. Grinnell, J. The niche-relationships of the California thrasher. *Auk* **34**, 427–433 (1917).
38. Bock, W. J. Concepts and methods in ecomorphology. *J. Biosci.* **19**, 403–413 (1994).
39. Grant, P. R. *Ecology and Evolution of Darwin's Finches* (Princeton Univ. Press, 1999).
40. Wilman, W. et al. EltonTraits 1.0: species-level foraging attributes of the world's birds and mammals. *Ecology* **95**, 2027 (2014).
41. Jetz, W., Thomas, G. H., Joy, J. B., Hartmann, K. & Mooers, A. O. The global diversity of birds in space and time. *Nature* **491**, 444–448 (2012).
42. Ricklefs, R. E. & Travis, J. A morphological approach to the study of avian community organization. *Auk* **97**, 321–338 (1980).
43. Cooney, C. R. et al. Mega-evolutionary dynamics of the adaptive radiation of birds. *Nature* **542**, 344–347 (2017).
44. Peters, R. H. *The Ecological Implications of Body Size* Vol. 2 (Cambridge Univ. Press, 1983).
45. Sugihara, G. Minimal community structure: an explanation of species abundance patterns. *Am. Nat.* **116**, 770–787 (1980).
46. Harvey, P. H. & Pagel, M. D. *The Comparative Method in Evolutionary Biology* (Oxford Univ. Press, 1991).
47. Mahler, D. L., Ingram, T., Revell, L. J. & Losos, J. B. Exceptional convergence on the macroevolutionary landscape in island lizard radiations. *Science* **341**, 292–295 (2013).
48. Moen, D. S., Morlon, H. & Wiens, J. J. Testing convergence versus history: convergence dominates phenotypic evolution for over 150 million years in frogs. *Syst. Biol.* **65**, 146–160 (2016).
49. Muschick, M., Indermaur, A. & Salzburger, W. Convergent evolution within an adaptive radiation of cichlid fishes. *Curr. Biol.* **22**, 2362–2368 (2012).
50. Mazel, F. et al. Prioritizing phylogenetic diversity captures functional diversity unreliably. *Nat. Commun.* **9**, 2888 (2018).
51. Naeem, S., Duffy, J. E. & Zavaleta, E. The functions of biological diversity in an age of extinction. *Science* **336**, 1401–1406 (2012).
52. Sekercioğlu, Ç., Wenny, D. G. & Whelan, C. J. *Why Birds Matter: Avian Ecological Function and Ecosystem Services* (Univ. of Chicago Press, 2016).
53. Derryberry, E. P. et al. Lineage diversification and morphological evolution in a large-scale continental radiation: the Neotropical ovenbirds and woodcreepers (Aves: Furnariidae). *Evolution* **65**, 2973–2986 (2011).
54. Ricklefs, R. E. Passerine morphology: external measurements of approximately one-quarter of passerine bird species. *Ecology* **98**, 1472 (2017).
55. Dunning, J. B. *CRC Handbook of Avian Body Masses* (CRC Press, 1993).
56. Burin, G., Kissling, W. D., Guimarães, P. R.Jr., Şekercioğlu, Ç. H. & Quental, T. B. Omnivory in birds is a macroevolutionary sink. *Nat. Commun.* **7**, 11250 (2016).
57. del Hoyo, J, Elliott, A, Sargatal, J, Christie, D. A. & de Juana, E. *Handbook of the Birds of the World* (Lynx Edicions, 1997).
58. Remsen, J. V. & Robinson, S. K. A classification scheme for foraging behaviour of birds in terrestrial habitats. *Stud. Avian Biol.* **13**, 144–160 (1990).
59. Croxall, J. P. *Seabirds: Feeding Ecology and Role in Marine Ecosystems* (Cambridge Univ. Press, 1987).
60. Ashmole, N. P. in *Avian Biology* Vol. 1 (eds Farner, D. S. et al.) 223–286 (Academic Press, 1971).
61. Fitzpatrick, J. W. Form, foraging behavior, and adaptive radiation in the Tyrannidae. *Ornithol. Monogr.* **36**, 447–470 (1985).
62. Hackett, S. J. et al. A phylogenomic study of birds reveals their evolutionary history. *Science* **320**, 1763–1768 (2008).
63. Drummond, A. J. & Rambaut, A. BEAST: Bayesian evolutionary analysis by sampling trees. *BMC Evol. Biol.* **7**, 214 (2007).
64. *ArcGIS Desktop: Release 10.3* (Environmental Systems Research Institute, 2014).
65. Breiman, L. Random forests. *Mach. Learn.* **45**, 15–32 (2001).
66. R Core Team. *R: A Language and Environment for Statistical Computing* (R Foundation for Statistical Computing, 2015).
67. Liaw, A. & Wiener, M. Classification and regression by randomForest. *R News* **2**, 18–22 (2002).
68. Grundler, M. & Rabosky, D. L. Trophic divergence despite morphological convergence in a continental radiation of snakes. *Proc. Biol. Sci.* **281**, 20140413 (2014).
69. Rabosky, D. L. et al. BAMMtools: an R package for the analysis of evolutionary dynamics on phylogenetic trees. *Methods Ecol. Evol.* **5**, 701–707 (2014).
70. Rabosky, D. L. et al. Rates of speciation and morphological evolution are correlated across the largest vertebrate radiation. *Nat. Commun.* **4**, 1958 (2013).
71. Nosil, P. & Harmon, L. J. in *Speciation and Patterns of Diversity* (eds Butlin, R. et al.) 127–154 (Cambridge Univ. Press, 2009).
72. Rayner, J. M. V. in *Current Ornithology* Vol. 5 (ed. Johnston, R. F.) 1–66 (Springer, 1988).
73. Revell, L. J. Size-correction and principal components for interspecific comparative studies. *Evolution* **63**, 3258–3268 (2009).
74. Revell, L. J. phytools: an R package for phylogenetic comparative biology (and other things). *Methods Ecol. Evol.* **3**, 217–223 (2012).
75. Sidlauskas, B. Continuous and arrested morphological diversification in sister clades of characiform fishes: a phylomorphospace approach. *Evolution* **62**, 3135–3156 (2008).
76. Stayton, C. T. The definition, recognition, and interpretation of convergent evolution, and two new measures for quantifying and assessing the significance of convergence. *Evolution* **69**, 2140–2153 (2015).
77. Holt, B. G. et al. An update of Wallace's zoogeographic regions of the world. *Science* **339**, 74–78 (2013).

Acknowledgements

We thank numerous field biologists and explorers who collected and prepared the specimens used in this study. We thank the Natural History Museum, the American Museum of Natural History and 63 other research collections for providing access to specimens. Illustrations are reproduced with permission of Lynx Edicions. Financial support was received from a Royal Society University Research Fellowship (A.L.P.); a PhD studentship funded by the University of Oxford Clarendon Fund and the US–UK Fulbright Commission (C.S.); and Natural Environment Research Council grant nos. NE/I028068/1 and NE/P004512/1 (J.A.T.). Secondary sources of funding are listed in the Supplementary Information, along with a complete list of individuals and institutions that contributed directly to data collection, logistics and specimen access.

Author contributions

J.A.T. and A.L.P. conceived and coordinated the study. J.A.T., A.L.P., C.S., E.T.M. and U.R. designed the study. C.S., A.L.P., T.P.B., B.G.F., U.R., C.H.T., B.C.W., N.S. and J.A.T. compiled the morphological, ecological and geographical data. A.L.P. led the analyses. All authors contributed to the writing of the manuscript.

Competing interests

The authors declare no competing interests.

Additional information

Extended data is available for this paper at https://doi.org/10.1038/s41559-019-1070-4.

Supplementary information is available for this paper at https://doi.org/10.1038/s41559-019-1070-4.

Correspondence and requests for materials should be addressed to A.L.P. or J.A.T.

Reprints and permissions information is available at www.nature.com/reprints.

Publisher's note Springer Nature remains neutral with regard to jurisdictional claims in published maps and institutional affiliations.

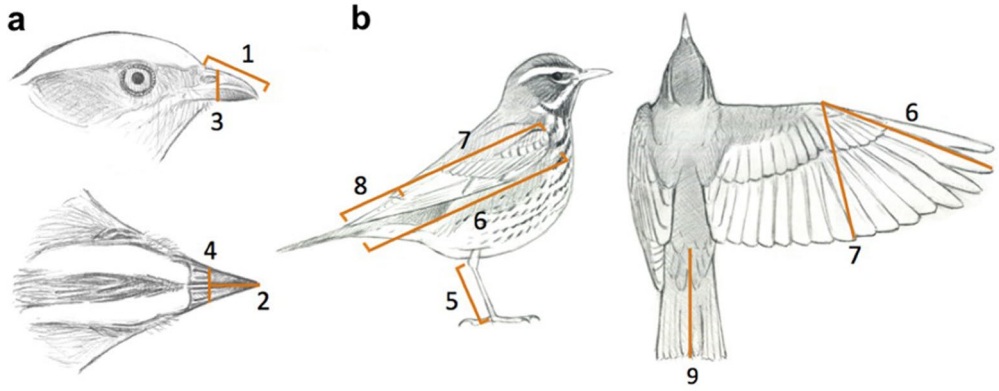

Extended Data Fig. 1 | Diagram of linear measurements of avian morphology. a, Resident frugivorous tropical passerine (fiery-capped manakin, *Machaeropterus pyrocephalus*) showing four beak measurements: (1) beak length measured from tip to skull along the culmen; (2) beak length measured from the tip to the anterior edge of the nares; (3) beak depth; (4) beak width. **b**, Insectivorous migratory temperate-zone passerine (redwing, *Turdus iliacus*) showing five body measurements: (5) tarsus length; (6) wing length from carpal joint to wingtip; (7) secondary length from carpal joint to tip of the outermost secondary; (8) Kipp's distance, calculated as wing length minus first-secondary length; (9) tail length. Analyses exclude Kipp's distance, and thus include 8 traits shown here (plus body mass, making 9 traits in total). Illustration by Richard Johnson.

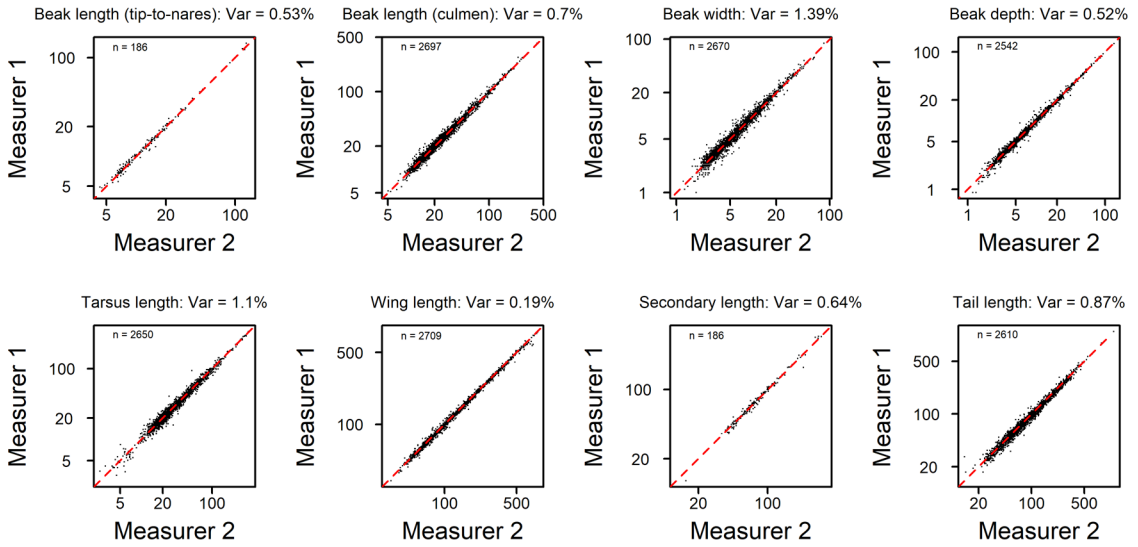

Extended Data Fig. 2 | Repeatability of avian morphological trait measurements. Data points show replicate measurements taken by different researchers on the same museum specimens for a subset of our global dataset ($n = 2752$ specimens of $n = 2523$ species). Points falling along the 1:1 line indicate a perfect correspondence between measurers. The % of total trait variance (Var) occurring between measurers within specimens is shown. The number of specimens varies across traits and is indicated in the top left of each plot.

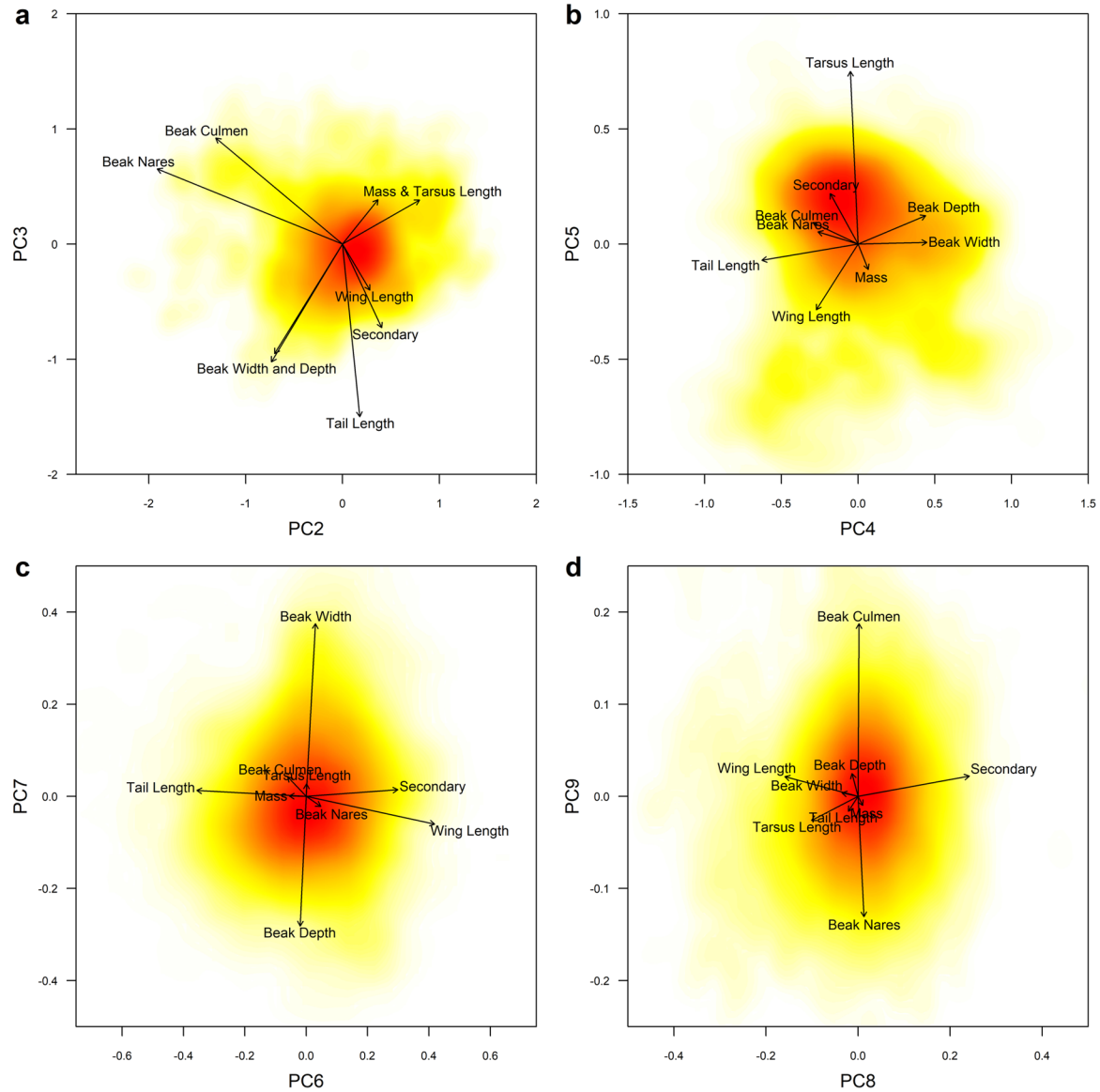

Extended Data Fig. 3 | Trait loadings along principal component (PC) dimensions based on all 9 phenotypic traits. Results are shown for PC axes representing variation in shape, and thereby excluding PC1 which represents variation in body size. Colours indicate the increasing density of species (from yellow to red) on each 2-dimensional plane (n =9,963 species). See Supplementary Table 3 for trait loadings.

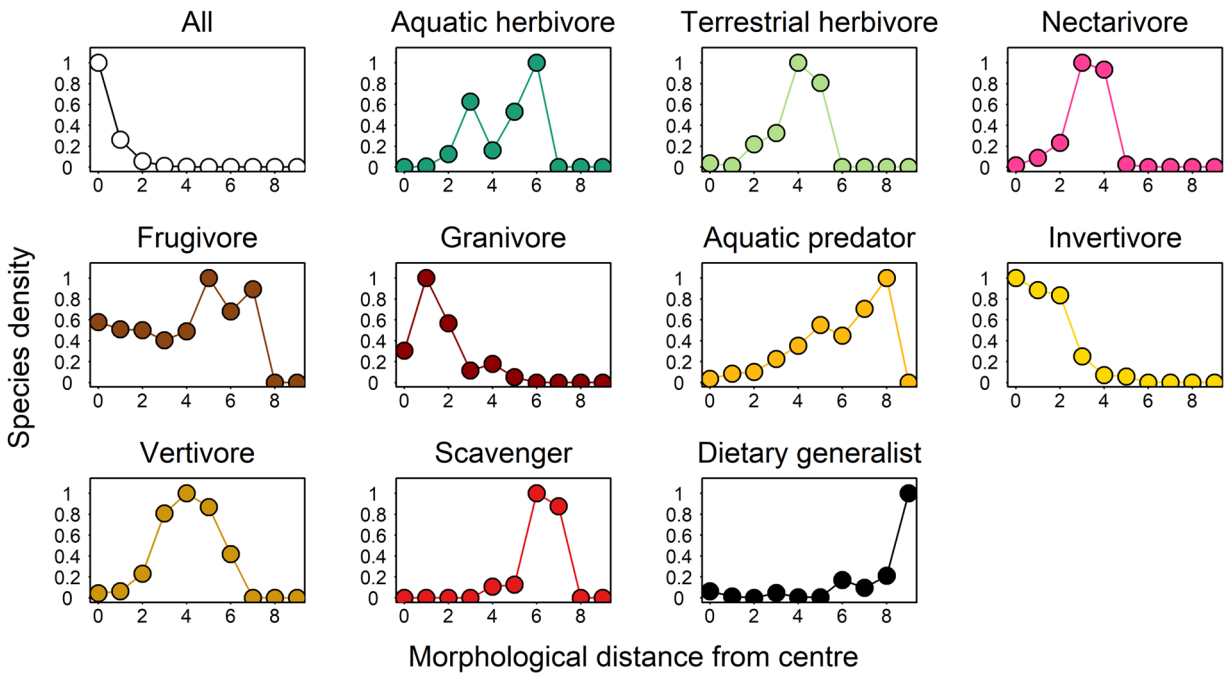

Extended Data Fig. 4 | Density profiles through multidimensional morphospace. The relative density of species with distance from the centroid of nine-dimensional morphospace is calculated for concentric shells of 1-unit diameter. Density is shown for all species (n = 9,963) and each trophic niche separately.

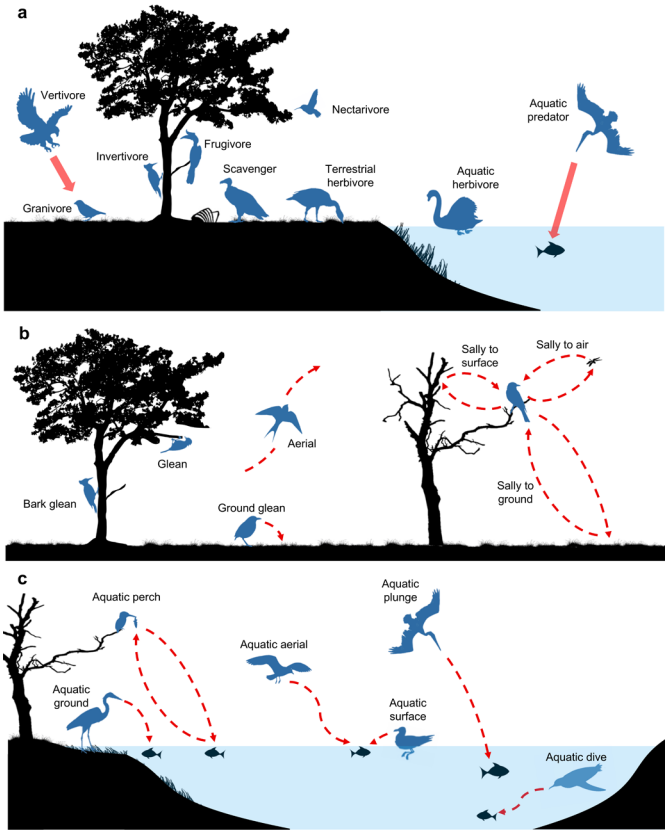

Extended Data Fig. 5 | Avian trophic niches and foraging niches. Silhouettes depict archetypal species belonging to (**a**) nine specialist trophic niches, (**b**) seven major foraging niches used by terrestrial invertivores, and (**c**) six major foraging niches used by aquatic predators. Foraging niches for the remaining seven specialist trophic niches are less diverse and are not shown. See Supplementary Table 4 for a full list and description of trophic and foraging niches. Bird silhouettes were generated directly from published illustrations with permission of Lynx Edicions (https://www.hbw.com/) or downloaded from online repositories without restrictions on use: http://phylopic.org/image/6da653ca-1baa-4852-b9db-aff15404cbf7/ http://www.clker.com/cliparts/f/7/9/a/11949848182045168189eagle_01.svg.med.png http://phylopic.org/image/05cd7d8c-6b2c-4b97-b7b8-053559019eeb/.

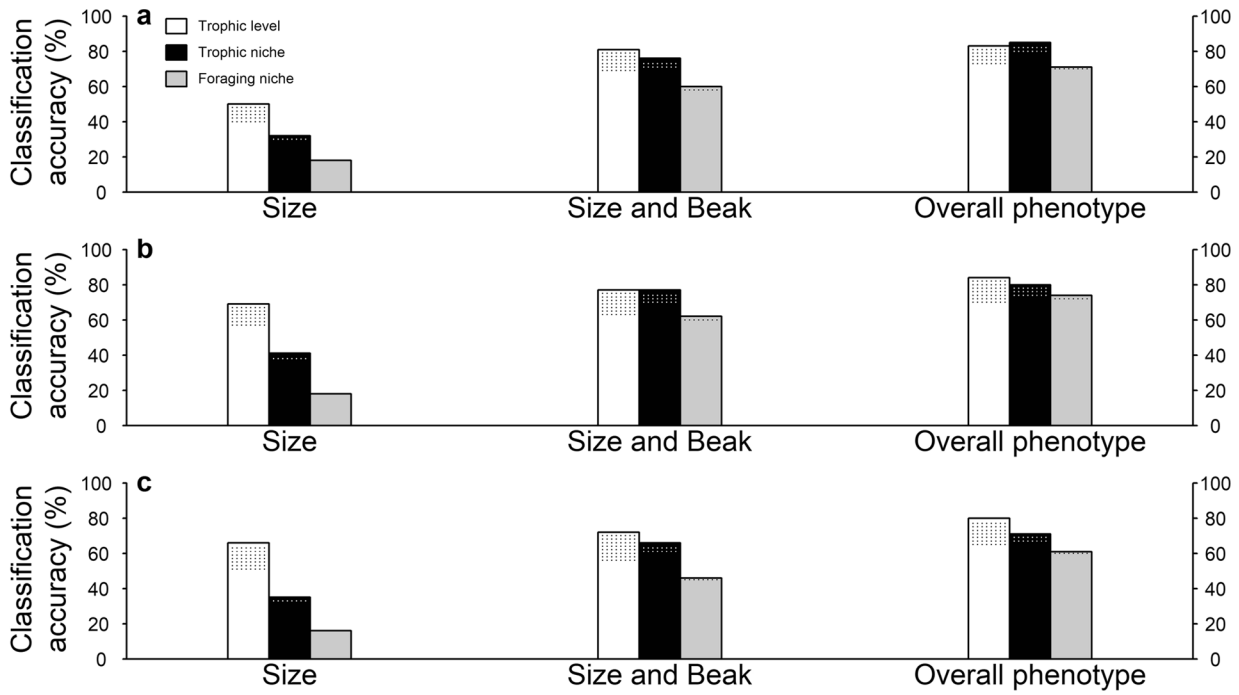

Extended Data Fig. 6 | Classification accuracy (%) using alternative classification algorithms. Predictions of species trophic levels, trophic niches and foraging niches using (**a**) Random Forest, (**b**) Mixture Discriminant Analysis, and (**c**) Linear Discriminant Analysis for all birds ($n = 9{,}963$ species) on the basis of body size (mass), size and beak traits, or the full nine-dimensional morphospace. Stippling indicates improvement in predictive accuracy after omitting omnivores and foraging generalists (see Methods).

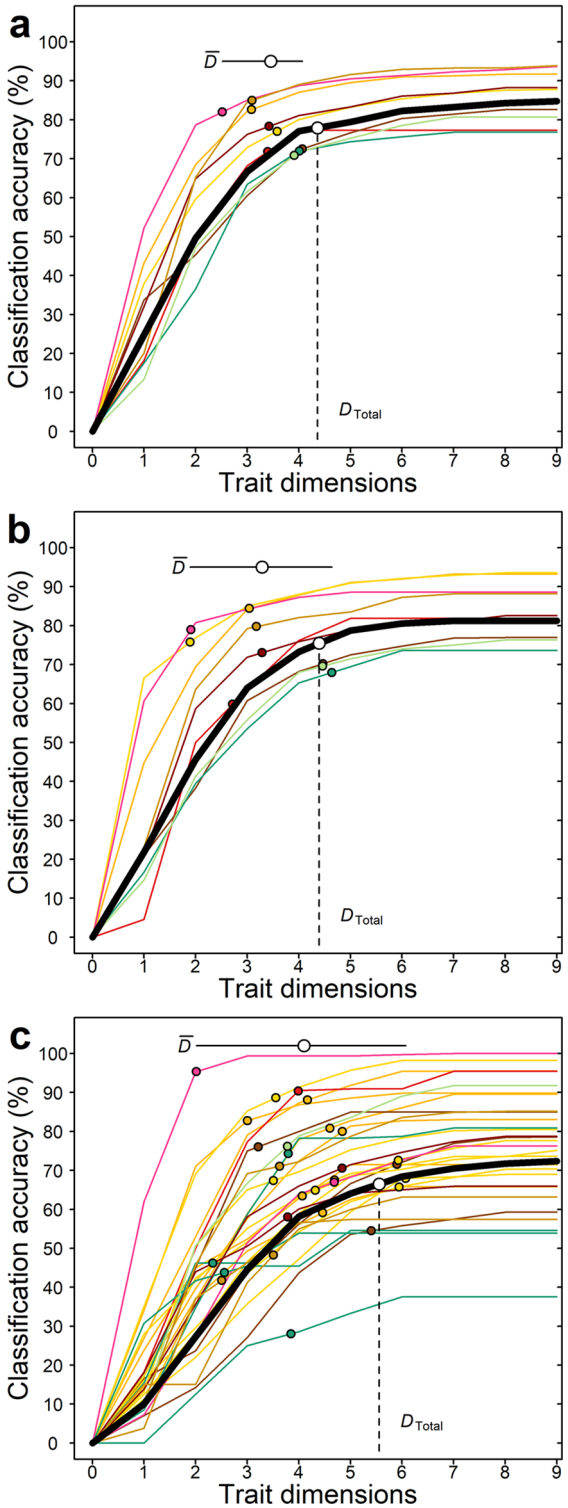

Extended Data Fig. 7 | Intermediate dimensionality of avian niche space. Accuracy curves indicate the maximum predictability of (**a-b**) trophic and (**c**) foraging niches in morphospaces consisting of different numbers of trait dimensions. Results are shown for a morphospace based on (**a**,**c**) standard and (**b**) phylogenetic principal components analysis. Accuracy is shown for individual niches (colours matching those depicted in Fig. 3) and total niche space (black, D_{Total}). Points indicate the level of niche dimensionality (D) according to Levene's index. Horizontal bar shows the mean ($\bar{D}$) and range in dimensionality estimates for each niche.

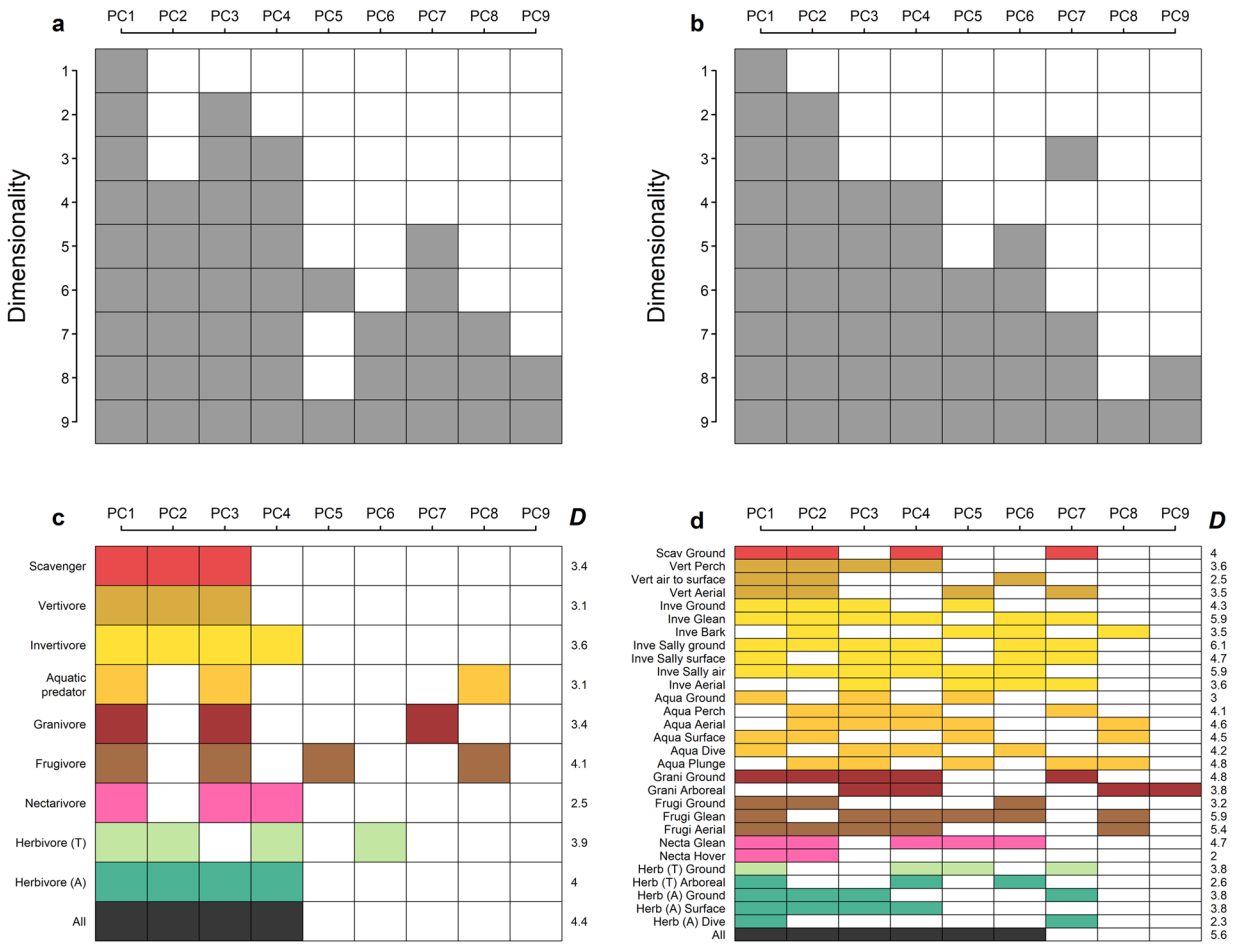

Extended Data Fig. 8 | The dimensionality of avian trophic and foraging niches. a-b, The identity of the trait dimensions best describing (**a**) trophic and (**b**) foraging niches for different levels of dimensionality. **c-d**, estimates of dimensionality (*D*) according to Levene's index for (**c**) trophic niches and (**d**) foraging niches. Each niche is given separately, and with all niches combined ('All'), along with the identity of the principal component (PC) dimensions (coloured squares) that best predict the niche.

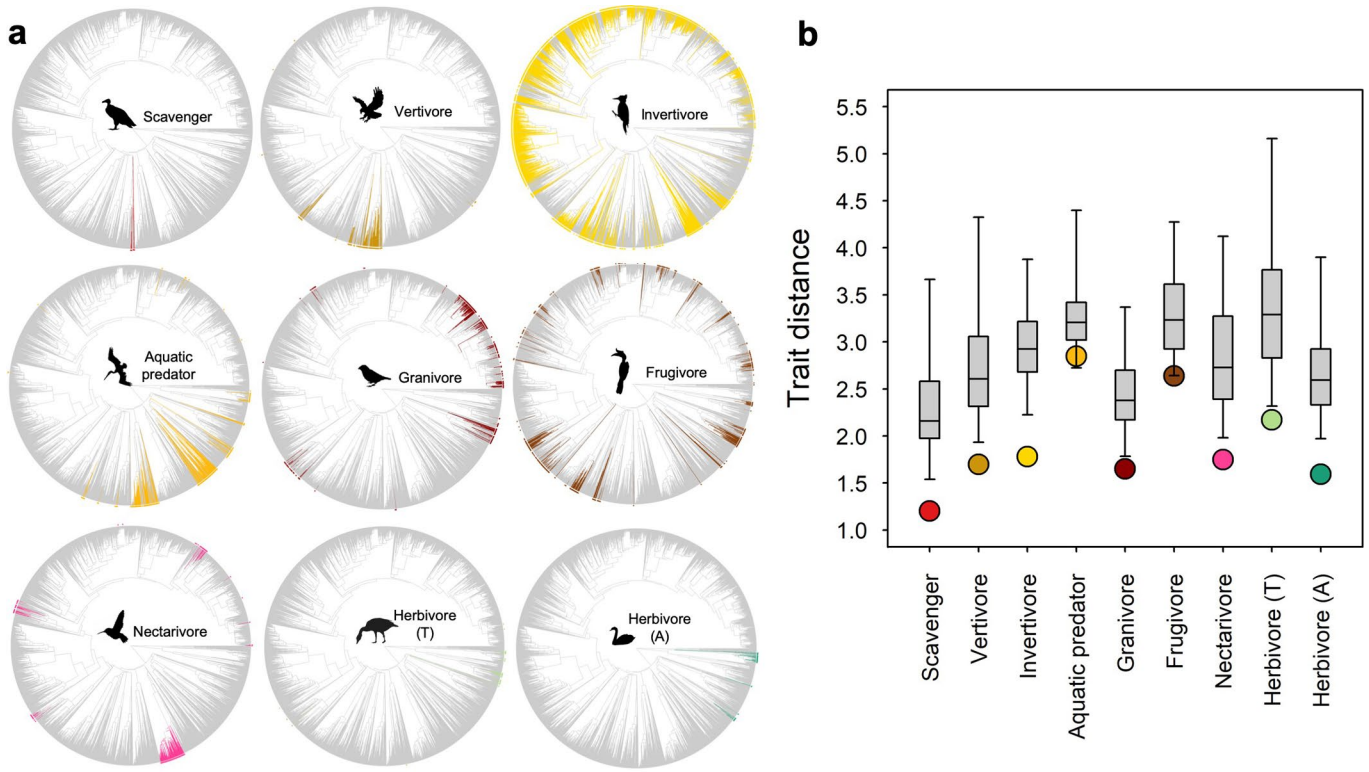

Extended Data Fig. 9 | Non-random trait packing within avian trophic niches. a, Phylogenetic distribution of avian trophic niches across the complete avian tree ($n = 9{,}963$ species) with species lacking genetic data inserted according to taxonomic constraints[41]. Tips and internal branches connected by species sharing the same trophic niche are highlighted across the avian evolutionary tree. **b**, Mean pairwise trait distance between species in each trophic niche (points) is less than expected due to phylogenetic relatedness, based on species with both morphological and genetic data ($n = 6{,}666$). Box and whiskers show 50% interquartile range and 95% confidence interval of mean pairwise trait distances expected under an evolutionary null model. This null model incorporates a multi-rate process of Brownian trait evolution whereby rates of evolution can vary both across lineages and over time. Bird silhouettes were generated directly from published illustrations with permission of Lynx Edicions (https://www.hbw.com/) or downloaded from online repositories without restrictions on use: http://phylopic.org/image/6da653ca-1baa-4852-b9db-aff15404cbf7/ http://www.clker.com/cliparts/f/7/9/a/1194984818204516818 9eagle_01.svg.med.png http://phylopic.org/image/05cd7d8c-6b2c-4b97-b7b8-053559019eeb/.

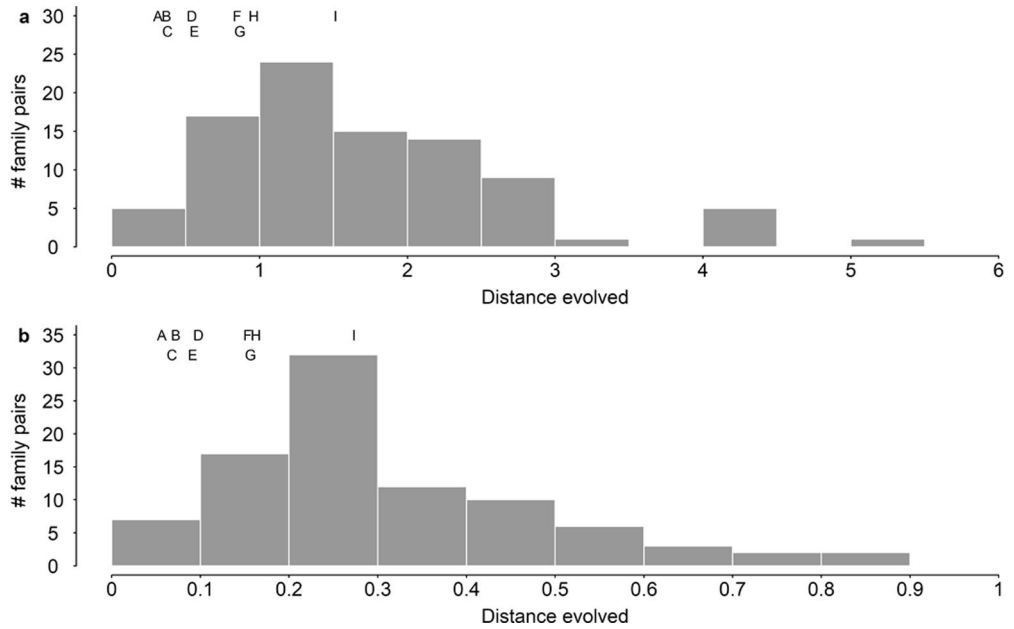

Extended Data Fig. 10 | The distance across morphospace independently evolved by phenotypically matched pairs of avian families. We calculated the average phenotypic distance evolved by each clade since they last shared a common ancestor with their phenotypically matched family ($n = 91$ pairs). Distances are expressed in (**a**) raw morphological units (trait axes scaled to unit variance) and (**b**) as a proportion of the total span of morphospace. On average, each clade within a matched family pair has independently evolved a distance equivalent to one-third of the total span of morphospace. For comparison, the 9 matched family pairs that are also sister clades (that is each other's closest relative) have each on average evolved a distance equivalent to only ~10% of the total span of morphospace. Position of letters indicate the average distance evolved by families within sister clades: (A) Cettiidae-Phylloscopidae, (B) Cardinalidae-Thraupidae, (C) Emberizidae-Passerellidae, (D) Phalacrocoracidae-Sulidae, (E) Odontophoridae-Phasianidae, (F) Strigidae-Tytonidae, (G) Ardeidae-Threskiornithidae, (H) Cacatuidae-Psittacidae, (I) Accipitridae-Cathartidae.

nature research

Corresponding author(s): Dr Joseph Tobias

Last updated by author(s): 2019/11/11

Reporting Summary

Nature Research wishes to improve the reproducibility of the work that we publish. This form provides structure for consistency and transparency in reporting. For further information on Nature Research policies, see Authors & Referees and the Editorial Policy Checklist.

Statistics

For all statistical analyses, confirm that the following items are present in the figure legend, table legend, main text, or Methods section.

n/a	Confirmed
☐	☒ The exact sample size (*n*) for each experimental group/condition, given as a discrete number and unit of measurement
☐	☒ A statement on whether measurements were taken from distinct samples or whether the same sample was measured repeatedly
☐	☒ The statistical test(s) used AND whether they are one- or two-sided *Only common tests should be described solely by name; describe more complex techniques in the Methods section.*
☐	☒ A description of all covariates tested
☐	☒ A description of any assumptions or corrections, such as tests of normality and adjustment for multiple comparisons
☐	☒ A full description of the statistical parameters including central tendency (e.g. means) or other basic estimates (e.g. regression coefficient) AND variation (e.g. standard deviation) or associated estimates of uncertainty (e.g. confidence intervals)
☐	☒ For null hypothesis testing, the test statistic (e.g. *F*, *t*, *r*) with confidence intervals, effect sizes, degrees of freedom and *P* value noted *Give P values as exact values whenever suitable.*
☐	☒ For Bayesian analysis, information on the choice of priors and Markov chain Monte Carlo settings
☐	☒ For hierarchical and complex designs, identification of the appropriate level for tests and full reporting of outcomes
☐	☒ Estimates of effect sizes (e.g. Cohen's *d*, Pearson's *r*), indicating how they were calculated

Our web collection on statistics for biologists contains articles on many of the points above.

Software and code

Policy information about availability of computer code

Data collection	No software was used to collect the data
Data analysis	Data was analysed using: 'R' v 3.5.2, 'ArcMap' v 10.3, 'BAMM' v 2.5.0 and 'BEAST' v 1.6.1

For manuscripts utilizing custom algorithms or software that are central to the research but not yet described in published literature, software must be made available to editors/reviewers. We strongly encourage code deposition in a community repository (e.g. GitHub). See the Nature Research guidelines for submitting code & software for further information.

Data

Policy information about availability of data

All manuscripts must include a data availability statement. This statement should provide the following information, where applicable:

- Accession codes, unique identifiers, or web links for publicly available datasets
- A list of figures that have associated raw data
- A description of any restrictions on data availability

All geographic and phylogenetic data are publicly available. Morphological data and ecological niche assignments are provided in supplementary Database 1

Field-specific reporting

Please select the one below that is the best fit for your research. If you are not sure, read the appropriate sections before making your selection.

☐ Life sciences ☐ Behavioural & social sciences ☒ Ecological, evolutionary & environmental sciences

For a reference copy of the document with all sections, see nature.com/documents/nr-reporting-summary-flat.pdf

Ecological, evolutionary & environmental sciences study design

All studies must disclose on these points even when the disclosure is negative.

Study description	Statistical analysis of the relationship between morphological and ecological traits of birds and their evolutionary history.
Research sample	Quantitative measurements of 8 phenotypic traits for 9963 species Ecological niche assignments for 9963 species Published data on body mass, geographic ranges and phylogenetic relationships for 9963 species
Sampling strategy	Morphological measurements were obtained for all available bird species. An average of 5 individuals were measured per species to provide reliable mean species values.
Data collection	Morphological data obtained from measurements of live caught individuals and preserved museum skins. Ecological data obtained from the literature.
Timing and spatial scale	Spatial scale: Global. Data obtained from multiple institutions and museum collections worldwide Timing: Data is based on museum collections spanning the last ~200 years.
Data exclusions	No data was excluded from the analysis.
Reproducibility	No experiments were conducted.
Randomization	NA
Blinding	NA

Did the study involve field work? ☐ Yes ☒ No

Reporting for specific materials, systems and methods

We require information from authors about some types of materials, experimental systems and methods used in many studies. Here, indicate whether each material, system or method listed is relevant to your study. If you are not sure if a list item applies to your research, read the appropriate section before selecting a response.

Materials & experimental systems

n/a	Involved in the study
☒	☐ Antibodies
☒	☐ Eukaryotic cell lines
☒	☐ Palaeontology
☐	☒ Animals and other organisms
☒	☐ Human research participants
☒	☐ Clinical data

Methods

n/a	Involved in the study
☒	☐ ChIP-seq
☒	☐ Flow cytometry
☒	☐ MRI-based neuroimaging

Animals and other organisms

Policy information about studies involving animals; ARRIVE guidelines recommended for reporting animal research

Laboratory animals	No laboratory animals were used
Wild animals	Most data are from museum specimens. Some data are included from wild-caught birds that were not harmed during data collection and subsequently released into the wild. In all cases, birds were caught by mist-netting, a passive, non-invasive technique which does not harm the individual birds.
Field-collected samples	No samples were taken from the field
Ethics oversight	Natural Environment Research Council

Note that full information on the approval of the study protocol must also be provided in the manuscript.